ARTICLE

OBC
www.rsc.org/obc

Carbohydrate–protein interactions at interfaces: comparison of the binding of *Ricinus communis* lectin to two series of synthetic glycolipids using surface plasmon resonance studies †

P. Critchley * and G. J. Clarkson
Department of Chemistry, University of Warwick, Coventry, UK CV4 7AL.
E-mail: lonpobty@supanet.com

Received 18th June 2003, Accepted 18th September 2003
First published as an Advance Article on the web 16th October 2003

Two C-lactosyl lipids and the related C-galactosyl lipids have been synthesised and their binding to RCA_{120} plant lectin was compared with a second series of thiolactosylethoxyalkanes. The interactions were measured quantitatively in real time by surface plasmon resonance (BIAcore) at a range of concentrations and temperatures from 5 to 30 °C. The C-galactosyl lipid (1,3-dimethyl-5-[β-D-galactopyranosyl]-5-(4-octadecyloxybenzyl)pyrimidine-2,4,6-trione) bound much more weakly with a $K_A = 8.86 \times 10^5$ than the corresponding C-lactosyl lipid (1,3-dimethyl-5-[β-D-galactopyranosyl-(1 ⟶ 4)-β-D-glucopyranosyl]-5-(4-octadecyloxybenzyl)pyrimidine-2,4,6-trione) ($K_A = 2.31 \times 10^7$). The influence of the linker region of the two different series of lactosyl lipids was clearly demonstrated by the differences in the binding to RCA_{120} lectin. The changes in kinetic values and in the enthalpic and entropic contribution to the free energy of binding reflected the importance of the linker and the hydrocarbon anchor holding the synthetic glycolipids in the neomembrane.

Introduction

Specific molecular recognition is a fundamental mechanism involved in the hour to hour and day to day processes within living organisms, from viruses and bacteria to *homo sapiens*. In a large proportion of cases the first stage of this recognition involves comparatively weak binding forces between specific proteins and the carbohydrate moieties of glycoproteins or glycolipids, often located on the membrane of the cell surface.[1,2] Synthesis of appropriate saccharide analogues capable of controlling these interactions would provide pharmacological agents useful for the treatment of various infections and other diseases including cancer.

Much of the literature on carbohydrate–protein interactions has concentrated on the differences in structure of related saccharides binding to one or more lectins.

C-glycosides are potentially useful tools in glycobiological studies as they represent hydrolytically stable analogues of O-glycosides. Moreover, they have equivalent, if not improved, properties as glycosidase inhibitors,[3–5] substrates for glycoside transferases[3,6] and in the increased induction of protein expression.[7] These factors and advances made in their synthesis,[8] especially in aqueous media,[6,9,10] have promoted recent research work on C-glycosides. This paper describes the synthesis of two glycolipids (1,3-dimethyl-5-[β-D-galactopyranosyl-(1 ⟶ 4)-β-D-glucopyranosyl]-5-(4-octadecyloxybenzyl)pyrimidine-2,4,6,-trione and the *N*,*N*′-dimethyl malonamide open ring form based on the C-glycoside of lactose and two analogous C-galactose glycolipids and a comparison of the binding of these structures with that of a second series of thiolactosyl-ethoxyalkanes (thiolactosyl lipids). The glycolipids and thiolactosyl lipids were incorporated into a synthetic membrane (called a neomembrane composed of dipalmitoylphosphatidyl choline and between 5–10 mol% of the chosen glycolipid). The single layer neomembrane was deposited on the surface of an HPA hydrophobic chip and binding to a *Ricinus communis* agglutinin (RCA_{120}) was studied at a range of concentrations and at different temperatures. The SPR model used in this work and the synthesis of the thiolactosyl lipids has been described previously.[11] In the first series of compounds a C-glycoside bond links the saccharide to a dimethyl barbituric acid spacer whereas in the second series the linkage is a thio bond to a hydrophilic linker of ethylene glycol groups (Fig. 1). The binding experiments were designed to investigate some of the minor differences in structure, particularly in the linker region of the molecules, and the effect of temperature on the specific molecular interactions between the same carbohydrates immobilised at a neomembrane interface and the same lectin in solution. The binding events at a synthetic membrane were followed using a BIAcore 2000 instrument. The kinetic values and the thermodynamic parameters calculated showed that both the linker and the hydrocarbon chain anchor played an important role in determinimg the amount of complex formed and its stability.

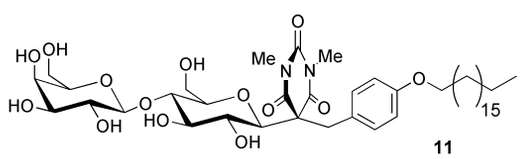

(a) lactose ligand — barbituric acid linker — hydrocarbon anchor

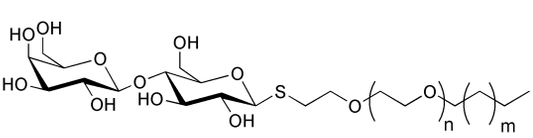

(b) lactose ligand — ethylene glycol linker — hydrocarbon anchor

	22	23	24	25	26	27
n	1	2	1	2	1	2
m	7	7	9	9	15	15

Fig. 1 (a) Cartoon of C-glycolipid structure (compound **11**) and (b) the thioglycolipids (compounds **22**–**27**) that shows the ligand, the linker and the anchor regions of the molecules.

There are many factors that influence: (a) whether specific molecular recognition can occur at an interface, and (b) whether the amount of binding is sufficient to trigger a relevant

† The authors would like to dedicate this paper to Professor D. H. G. Crout on his retirement in September 2003 without whose encouragement the work would not have been published.

DOI: 10.1039/b306784j

biological cascade such as host defence mechanisms, fertilisation, cell division, or differentiation.

Some of the factors involved in binding are specific whereas others are not. Equilibrium association constants for the binding of simple carbohydrates to proteins in a 1 : 1 complex in solution are weak (K_A = 10^4 M^{-1}). Specific recognition is enhanced by cluster formation where a group of glycolipid ligands can aggregate within a membrane to provide a multiple binding site for a polyvalent protein or particle with several copies of the binding domain.[12,13] This assumes that the ligand molecules are not rigidly bound to the surface by short covalent linkers that may make them inaccessible to a protein. The resultant multivalent binding is strong (K_A of 10^6 to 10^9 M^{-1}) and this is very necessary for adherence where dynamic flow takes place and hydrodynamic shear could remove proteins from membranes where weak binding of $<10^4$ was involved. Further in a second phase of binding, stronger associations are formed through protein–protein interactions or by fusion of a protein or a particle (*e.g.* a virus) with the host cell membrane.[14,15] Whilst clustering of molecules within a membrane by lateral diffusion can allow specific multivalent interactions to occur between molecules this is not the only way that strong binding can be achieved. Some of the more important factors that play a role in binding are as follows. The concentration of glycolipid ligand in a membrane, the composition of the surrounding lipids, the length of the spacer holding the glycoside away from the lipid membrane allowing rotation and deformation of the head group to occur, and the effects of pH and temperature.[16] The way that a ligand is presented at an interface can influence the strength of interaction with an appropriate lectin on a scale from 0–100%.[17] There are many unexplained examples in the biological literature of the effect of different lipid structures, that are either part of a glycolipid or are part of the phospholipid microenvironment, changing the degree of interaction between the glycoside (bound to the lipid) and a lectin[16,18] or enzyme.[19]

A further complication of examining binding events at interfaces is that non-specific binding of proteins occurs at apolar sites. Many proteins have hydrophobic regions that will bind non-specifically to hydrophobic surfaces[20] and some bind to charged surfaces of membranes.[21] Recent work has shown that the introduction of ethylene glycol oligomers or other polar molecules at an interface can significantly reduce the non-specific binding and facilitate specific interactions.[22]

A number of papers have been published to explain the high binding at interfaces compared with that measured by methods that use solution systems for binding measurements.[16,23] The explanations offered in the literature do not fit all of the observations and it seems likely that some of the numbers for binding constants may result from artefacts introduced by the model chosen and the experimental technique used to make the measurements.[24] Most of the early work was done using agglutination techniques with cells or liposomes. These techniques measured equilibrium situations after many minutes to hours and often used markers such as fluorescent labels that may modify a response.[16] More recently techniques such as titration microcalorimetry,[25] and surface plasmon resonance[26] have been used to follow binding reactions in real time. Surface plasmon resonance in the form of a BIAcore instrument is particularly useful to study molecular interactions because it allows one to follow a reaction over a period of many seconds. No label is required so native molecules can be used without modification. Further, the concentration of the analyte is constant and a relatively large volume of analyte, compared with the volume of the reaction cell, is passed over the low concentration of ligand bound to a surface. Therefore, a bimolecular second order reaction behaves as if it were a pseudo-first order reaction simplifying the mathematics. The forces involved in specific molecular interactions in aqueous solution include dipole–dipole interactions (including induced dipoles), dispersion interactions and hydrogen bonding. Water as the solvent has a major effect on interactions and it is the loss of favourable interactions between solutes and water that is compensated by the favourable interactions between solutes when a complex is formed. Many organic compounds dissolved in water produce an energetically unfavourable pertubation to the structure of water (the hydrophobic interaction). When a ligand–lectin complex is formed at least part of this unfavourable pertubation of water is relieved and the free energy of the bound system is consequently lower than that of the unbound state because solvated water molecules are returned to the bulk phase.[24] Water molecules can be trapped when a complex is formed and this water can provide additional hydrogen bonds that stabilize the complex and can account for the large enthalpic contribution to the free energy of binding (-90 kJ mol^{-1}).[27] The vibrational states of both free and bound molecules are influenced particularly by temperature that changes the collision rate. Moreover, as the chemical environment changes the activation energies of the reacting molecules are influenced. The chemical environment can be influenced experimentally by comparing different chemical structures in a series and by factors such as pH, temperature and solvent.[28]

Results and discussion

Two different series of novel glycolipid have been synthesised and used as models to examine the influence of the linker unit on the binding to the lectin *Ricinus communis* agglutinin 120 kDa (RCA_{120}). The linker is present between the lactose residue and the long-chain hydrocarbon that acts as an anchor designed to hold the glycolipid in a neomembrane (Fig. 1).

Chemical synthesis

The first set of compounds was synthesised by a simple five stage sequence of reactions (Scheme 1). The anchor part of the molecule was formed by alkylation of 4-hydroxybenzaldehyde **1** with 1-bromooctadecane[29] followed by mild reduction of the aldehyde group **2** with sodium borohydride.[30] Treatment of the phenyl methanol compound **3** obtained with thionyl chloride gave the 1-chloromethyl-4-octadecyloxybenzene **4**.[31] Galactose or lactose was added to *N*,*N*′-dimethylbarbituric acid **5** under mild alkaline conditions[32] (Scheme 2). The galactosyl barbiturate **6** and the lactosyl barbiturate **7** were reacted with 1-chloromethyl-4-octadecyloxybenzene **4** to give the required compounds **10** and **11** (Scheme 3). The cellobiosyl dimethylbarbituric acid derivative (compound **8**) and the maltosyl dimethylbarbituric acid **9** were prepared in a similar way and alkylated with **4** to produce the C-glycosyl lipids **12** and **13**. These compounds were used as negative controls in the binding experiments to check that the dimethyl barbituric acid linker and octadecylbenzyl anchor showed no binding to RCA_{120} lectin. The barbituric acid ring can be cleaved under mild alkaline conditions.[33,34] Treatment of the galactosyl or lactosyl compound with alkali opened the barbituric acid ring to yield *N*,*N*′-dimethylmalonamide derivatives (compounds **14** and **15**) (Scheme 4). The sugar protons resonated over a very small ppm range in the ^{1}H NMR and it was difficult to obtain an elemental

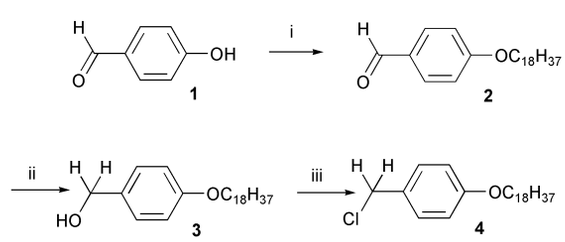

Scheme 1 Synthesis of the anchor part of the C-glycolipids compound **4**. *Reagents and conditions*: (i) $BrC_{18}H_{37}/K_2CO_3$/DMF, (ii) $NaBH_4$/MeOH, (iii) $SOCl_2$

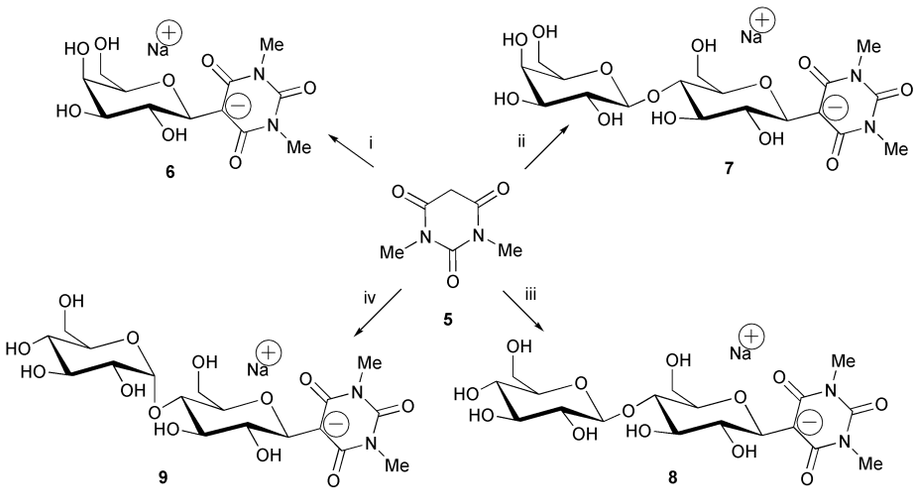

Scheme 2 Synthesis of the ligand and linker part of the C-glycolipids showing the reaction of *N,N′*-dimethylbarbituric acid **5** with (i) galactose, (ii) lactose, (iii) cellobiose and (iv) maltose, in $NaHCO_3$ (aq) to form compounds **6**, **7**, **8** and **9**.

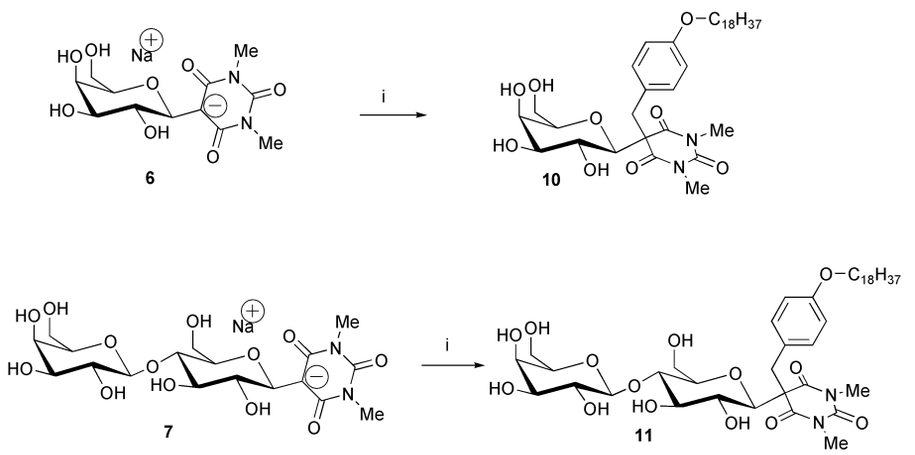

Scheme 3 Coupling of the C-galactosyl/linker **6** and C-lactosyl/linker **7** molecules to the anchor 1-chloromethyl-4-octadecylbenzene (**4**) in DMSO.

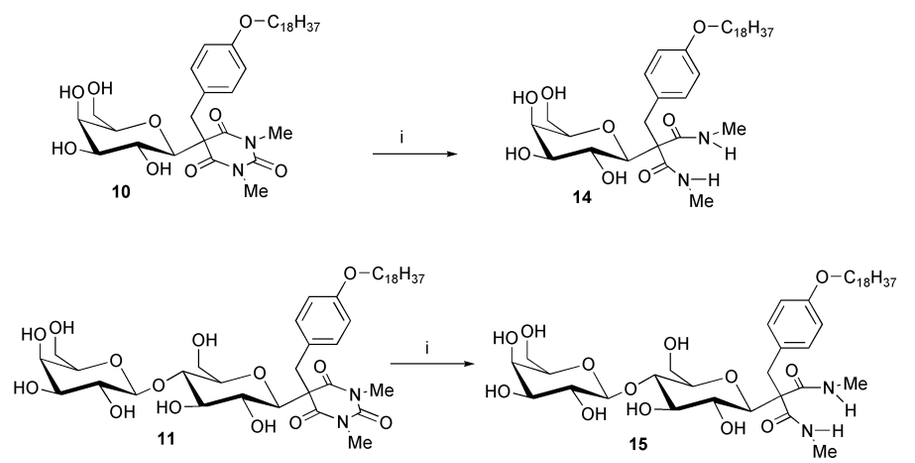

Scheme 4 Hydrolysis of the dimethylbarbituric acid linker of **10** and **11** with NaOH/THF/H_2O to form the dimethylmalonamides **14** and **15**, respectively.

analysis for the compounds with free hydroxyl groups (**10**–**15**). Therefore the compounds were fully characterised as their peracetates **16**–**21**.

It is known that by replacing the normal glycosidic oxygen bond with a carbon bond could change the conformation of the molecule and this may result in a different orientation of the sugars at the neomembrane surface.[35,36] The C-glycosides had a hydrophilic malonamide or a more hydrophobic barbituric acid group[33b] present adjacent to the sugar and this produced structures that were significantly different from the thioglycolipids with ethylene glycol spacers.

The synthesis of the second series of compounds (**22**–**27**) has been described.[11] In brief, α,ω-bifunctional dimers and trimers of ethylene glycol with a monochloro end-group were converted to the 2-(2-benzylsulfanylethoxy)ethanol or 2-[2-(2-benzylsulfanylethoxy)ethoxy]ethanol by a base catalysed reaction with benzyl thiol.[37] Reaction of the products with C_{10}, C_{12} and C_{18} 1-bromoalkanes in the presence of basic sodium iodide and a phase transfer catalyst gave the alkylated products.[38] Removal of the protecting benzyl group with sodium and liquid ammonia liberated the thiol group[39] for condensation with octa-*O*-acetyllactose. The condensation reaction was enabled with

Table 1 Binding of *Ricinus communis* agglutinin (RCA_{120}) at 298 K to the two series of synthetic glycolipids incorporated into a dipalmitoylphosphatidyl choline neomembrane

Glycolipid	k_a M^{-1} s^{-1}	k_d s^{-1}	K_A M^{-1}	K_D M [c]
10	9.21×10^3	1.04×10^{-2}	8.86×10^5	$1.13 (\pm 0.22) \times 10^{-7}$
11	1.03×10^5	4.45×10^{-3}	2.31×10^7	$4.33 (\pm 0.42) \times 10^{-8}$
14	NB [a]	NB	NB	NB
15	1.78×10^5	6.25×10^{-3}	2.84×10^7	$3.52 (\pm 0.31) \times 10^{-8}$
22 [b]	*5.58×10^3*	*1.16×10^{-3}*	*4.81×10^6*	*2.08×10^{-7}*
23 [b]	*1.76×10^3*	*1.77×10^{-3}*	*9.94×10^5*	*1.01×10^{-6}*
24	8.28×10^3	9.64×10^{-3}	8.59×10^5	$1.16 (\pm 0.12) \times 10^{-6}$
25	7.94×10^3	2.69×10^{-3}	2.95×10^6	$3.39 (\pm 0.21) \times 10^{-7}$
26	8.81×10^3	3.64×10^{-3}	2.42×10^6	$4.13 (\pm 0.29) \times 10^{-7}$
27	6.49×10^4	6.30×10^{-3}	1.03×10^7	$9.73 (\pm 0.34) \times 10^{-8}$

[a] NB No binding detected. [b] Compound **22** and **23** both failed to remain on the membrane and therefore the kinetic analysis is not valid for these two compounds. [c] Standard deviations for K_A are given in Table 2. The S.D. values for K_D are given in parentheses.

boron trifluoride etherate in dichloromethane to yield the protected glycolipids.[40] Treatment of each of the six acetates with sodium methoxide gave the deprotected lactosylthioethoxyalkane products (compounds **22**–**27**) that were purified separately by flash chromatography on silica. Some similar compounds have been described with a normal O-glycosidic linkage.[41] The effect of the linker and the length of the hydrocarbon chain in holding the model glycolipids on the surface of the sensor chip and any influence that different lengths of hydrocarbon chain may exert on the binding of the lectin was explored.

Biological results

We chose to design the experiment with C-glycolipid or thioglycolipid on the surface of an HPA chip to avoid the potential difficulty of aggregation of the glycolipid in solution (which would have made the interpretation of data that requires an accurate concentration term for the analyte) very difficult. Also, BIAcore recommend that the best results on the model 2000 are obtained with analytes of more than 10 kDa molecular weight. Advantages of the HPA chip over the CM5 chip (where molecules are covalently linked) and over the SA chip (where biotinylated analytes are deposited onto a streptavidin surface) are that the HPA chip allows mobility of ligands on the surface so that clusters can form by lateral difusion. Moreover, the chip is easily regenerated and the lipid/glycolipid ligands can be changed whereas the very tightly held biotinylated ligands and those covalently-linked to a CM5 chip cannot be exchanged. Details of the method of preparation of the glycolipid layers on the HPA chip surface and the development of the model have been described previously.[11]

In solution interactions RCA_{120} binds two galactosides, one on each face. In our experiments with galactolipids immobilised at a lipid interface there was no evidence of the second binding. Neomembranes could be used for several weeks with repeated regenerations with sodium hydroxide to remove any bound lectin. A 10 mol% of glycolipid ligand concentration in dipalmitoylphosphatidyl choline and low concentrations of RCA_{120} analyte (25–200 nM) were used under carefully controlled conditions for kinetic studies. Binding of RCA_{120} to the dipalmitoylphosphatidylcholine control was negligible and this was subtracted from all test runs. Neither C-cellobiosyl nor C-maltosyl lipids **12**, **13** showed any binding to RCA_{120}. Previous experiments showed that mass transfer was not a problem with flow rates of 20–30 μl min^{-1}.[11]

A typical sensorgram for the C-lactosyl lipid (compound **11**) is shown in Fig. 2. A comparison of the rates of association K_A and of dissociation k_d and the equilibrium constants K_A and K_D is given in Table 1.

The reaction may be expressed as A + B ⟶ AB.

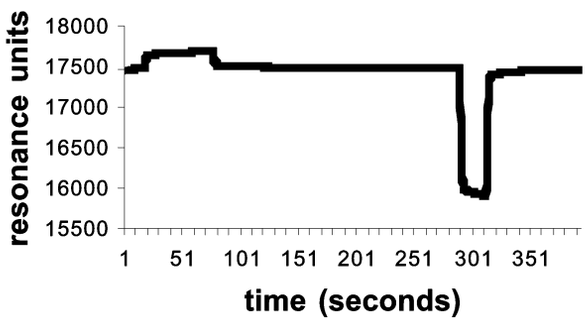

Fig. 2 Sensorgram of RCA_{120} binding to compound **11** showing the association phase (15–75 s), the dissociation phase (76–286 s) and the regeneration of the neomembrane with dilute alkali (287–384 s).

In BIAcore terms [AB] = the concentration of bound analyte A that is proportional to R_A the resonance response of a sensorgram at any given time t.

The free ligand concentration [B] is the difference between the total and bound ligand

$$[B_t] = [B_{t=0} - AB_t]$$

Therefore the total concentration of active immobilized ligand is obtained indirectly as it is saturated with analyte. The maximum response due to analyte binding R_{max} is proportional to total ligand concentration $[B_{t=0}]$. Also, $(R_{max} - R_{At})$ is proportional to the free ligand concentration $[B_t]$. The concentration of complex $[AB_t]$ formed and of $[B_t]$ the free ligand remaining can be expressed in terms of analyte response in the equation

$$d[AB]/dt = k_a[A][B] - k_d[AB] \quad (1)$$

In BIAcore terms this becomes

$$dR_A/dt = k_aC(R_{max} - R_A) - k_dR_A \quad (2)$$

C is the concentration of the injected analyte in moles (M).[42]

At equilibrium $dR_A/dt = 0$ and the equilibrium constant $K_A = k_a/k_d$.

Therefore

$$R_A/C = K_AR_{max} - K_AR_A$$

A plot of R_A/C against R_A is a Scatchard plot with a slope of $-1/K_D$ (Fig. 3)

We can rearrange eqn. (2) to give

$$dR_A/dt = k_aCR_{max} - (k_aC + k_d)R_A \quad (3)$$

Table 2 Thermodynamic parameters calculated at 298 K for both series of synthetic glycolipid

Compound	K_A M^{-1}	$\Delta G°$ kJ mol^{-1}	$\Delta H°$ kJ mol^{-1}	$\Delta S°$ J mol^{-1} K^{-1}
10	$8.86\ (\pm 0.30) \times 10^5$	−33.9	−62.3	−95
11	$2.31\ (\pm 0.12) \times 10^7$	−41.9	−7.64	+115
15	$2.84\ (\pm 0.13) \times 10^7$	−42.5	−10.8	+107
24	$8.59\ (\pm 0.26) \times 10^5$	−33.8	−17.3	+55
25	$2.95\ (\pm 0.25) \times 10^6$	−36.9	−49.3	−42
26	$2.42\ (\pm 0.12) \times 10^6$	−36.4	−59.5	−77
27	$1.03\ (\pm 0.17) \times 10^7$	−39.9	−35.7	+14

The values in parentheses after the K_A are the standard deviation for 12 measurements.

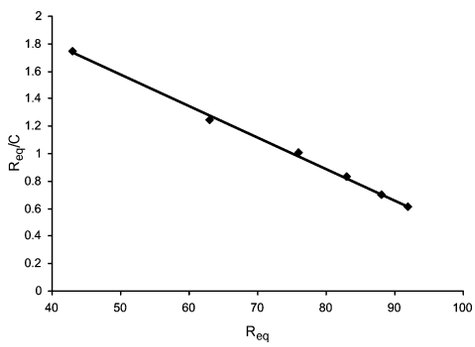

Fig. 3 A Scatchard plot of $R_{equilibrium}$/concentration of analyte against $R_{equilibrium}$ for compound **11**. The gradient = $-1/K_D = K_A = 2.33 \times 10^7$; compares with 2.31×10^7 average of 12 experiments (see Table 2 for the standard deviations).

The total response $R = R_I$ a refractive index component + R_L immobilised ligand component + R_A component for analyte bound and is a complex term. However, the derivatives dR_I/dt and $dR_L/dt = 0$ provided that ligand is not lost from the chip surface during the reaction. Therefore $dR/dt = dR_A/dt$

Substituting into eqn. (3) we obtain

$$dR/dt = \text{constant} - (k_a C + k_d)R$$

This equation can be used with several concentrations of analyte to find the k_{obs} values that are the gradient of a plot of dR/dt against R.

As $k_{obs} = k_a C + k_d$. a further plot of k_{obs} against concentration of analyte gives a straight line with a slope of k_a, the rate constant for association (Fig. 4).

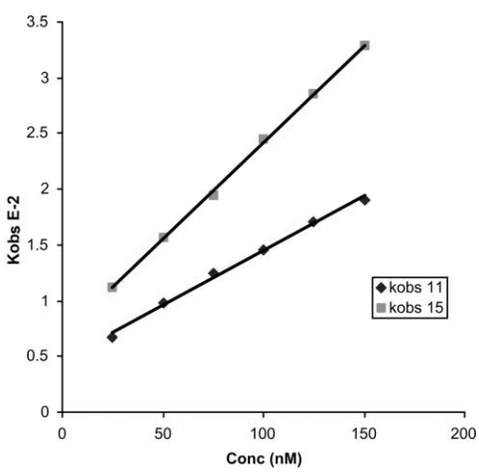

Fig. 4 A plot of k_{obs} against concentration of RCA_{120} for compound **11** ($k_{obs\ 11}$) and compound **15** ($k_{obs\ 15}$) The gradient $k_{a\ 11}$ is the association rate constant = 9.76×10^4 and the intercept is the dissociation rate constant $k_d = 7.08 \times 10^{-3}$. Therefore $K_A = k_a/k_d = 2.08 \times 10^7$. When the k_d from the sensorgram is used = 4.45×10^{-3}, then the $K_A = 2.19 \times 10^7$ that is closer to the average value in Table 1. The $k_a = 1.74 \times 10^5$ value for compound **15** with an intercept $k_d = 7.08 \times 10^{-3}$ giving a $K_A = 2.46 \times 10^7$. The value from the desorption sensorgram was $k_d = 6.25 \times 10^{-3}$ giving a $K_A = 2.78 \times 10^7$ much closer to the average value in Table 1.

When the injection of analyte finishes only buffer flows over the chip surface and the complex AB starts to dissociate. eqn. (3) can be rearranged to give

$$dR_A/dt = k_a C(R_{max} - R_A) - k_d R_A$$

Since there is no analyte flowing ($C \longrightarrow 0$) the equation can be simplified to

$$dR_A/dt = -k_d R_A$$

and values of k_d can be obtained from the dissociation phase of the sensorgram using the rate equation $\ln(R_{A1}/R_n) = k_d(t_n - t_1)$ where R_{A1} is the resonance at time t_1 when dissociation starts, R_n and t_n are values along the dissociation curve.

The data for the rate constants and the equilibrium constants at 25 °C are summarised in Table 1 and represent averages of between 5 and 14 separate experiments on each compound using five concentrations of lectin in each experiment. Standard deviations for K_A values are given in Table 2. The association constants K_A are orders of magnitude higher than the binding constant for free lactose [16] to RCA_{120} where $K_A = 3.8 \times 10^3$ M^{-1}

A comparison of the K_A figures shows that the binding of the C-galactosyl lipid (compound **10**) is 26 times weaker than the corresponding C-lactosyl lipid (compound **11**). A small favourable change in binding resulted when the dimethylbarbituric acid ring of the lactosyl compound was opened to form the *N*,*N*′-dimethyl malonamide **15**. The lactosyl lipid-RCA_{120} lectin complex with the open ring was more stable, ie it had a lower value for K_D that resulted largely from an increased rate of association. However, no binding was detected with the *N*,*N*′-dimethyl malonamide attached to galactose (**14**), contrary to our expectations. The concentrations of RCA_{120} used in all experiments, the pH of the buffer, the temperature range used in the experiments and the phospholipid used to make up the bulk of the neomembrane were the same. Moreover, the amount of ligand available in the neomembranes was very similar. The ligands represented a small fraction of the neomembrane (10 mol%) and therefore the environment around each ligand and its structure would determine the extent to which they were exposed at the membrane surface to allow binding to occur with RCA_{120} lectin (see similar examples in refs. 16, 18 and 19).

In the second series of compounds the thiolactosyl lipids there were suprising differences in the K_D resulting from changes in linker or spacer (between the thiolactose and the hydrocarbon chain) from three units down to two units of ethylene glycol. A comparison between two pairs of compounds (**24**, **25** and **26**, **27**) showed that removal of an ethylene glycol group reduced the K_D by more than an order of magnitude. Earlier work had shown that self-assembled monolayers terminated by three ethylene glycol groups showed less conformational variation than those terminated by six ethylene glycol groups.[43] There was a noticeable difference in the solubility of the compounds particularly those with octadecyl hydrocarbon chains as anchors. The compounds with three ethylene glycol groups were more easily formulated into liposomes than the

ones with two ethylene glycol groups that were less soluble. The exception to the change in K_D was the pair of compounds **22**, **23** with a decyl hydrocarbon tail. In these compounds the short hydrocarbon chain failed to hold the compounds sufficiently tightly in the membrane and at higher concentrations of RCA_{120} (>75 nM), the thiolactosyl lipid was removed from the surface as a ligand-lectin complex. This loss of thioglycolipid resulted in a lower signal at the end of an experiment compared to that at the start and the baseline decreased when experiments were repeated. The "kinetic data" found for these compounds has been included as an illustration of the artifacts that can be created by analysing sensorgrams that are not kinetically valid.

The values of K_A for each compound were measured at 5 °C intervals between 5 and 30 °C and analysed graphically by applying the van't Hoff isochore that relates variation in the equilibrium constant (K) with changes in the absolute temperature.

Thus, $\mathrm{d}\ln K/\mathrm{d}t = -\Delta H^\circ/RT^2$ where ΔH° is the enthalpy change and R is the gas constant. Integrating the equation gives

$$\ln K_2/K_1 = \Delta H^\circ/R(T_2 - T_1/T_1T_2)$$

A plot of $\log K$ against $1/T$ gives a straight line of slope $-\Delta H^\circ/2.303R$ (Fig. 5)

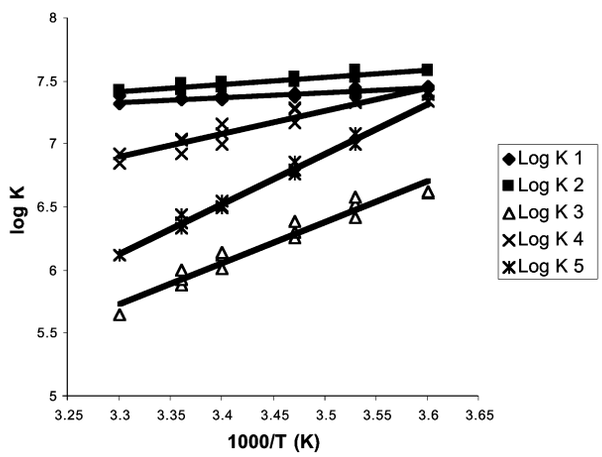

Fig. 5 A van't Hoff plot of log K_A against 1000/T. The almost parallel upper curves K_1 and K_2 represent compounds **11** and **15**, respectively; K_3 represents the galactosyl lipid compound **10** and K_4 and K_5 represent the thiolactosyl glycolipids compounds **26** and **27**, respectively. The curves with the lower gradient (compounds **11**, **15** and **26**) are the ones with a positive entropic contribution to the free energy of binding.

The average enthalpy change for each compound measured over the 25 °C range of temperature was used to find the change in free energy (ΔG°) and the entropy (ΔS°) of the reactions using the standard thermodynamic expressions:

$$\Delta G^\circ = -RT\ln K = \Delta H^\circ - T\Delta S^\circ$$

A summary of the thermodynamic results is shown in Table 2

The van't Hoff plot (Fig. 5) shows the relationship between the equilibrium constant for association and the absolute temperature. The reactions were all exothermic with an increase in K_A as the temperature was lowered. The gradient of each line is proportional to the change in enthalpy (ΔH°) and therefore as the gradient increases the enthalpic contribution to the free energy (ΔG°) of reaction is increased. Conversely, as the gradient decreases the enthalpic contribution is decreased. In the case of three of the compounds **10**, **25** and **26** the change in the entropic contribution is compensated for by the change in enthalpy. Similar thermodynamic parameters for the interaction of many different carbohydrates and lectins have been reviewed recently and in most of these examples there was a similar enthalpy-entropy compensation.[24] However, in our case some values for the entropy term (ΔS°) were positive because the free energy (ΔG°) was sometimes greater than the enthalpy term (ΔH°). Other authors observed positive entropy values when they measured the interaction of concanavalin A and pea lectin with various mannosides[44] and the binding of galactosides and lactose to *Erythrina corallodendron* lectin.[45] Such differences may reflect the difference in the technique of measuring the changes (see below). The values in the published work were calculated from titration microcalorimetry data that is known to include processes that do not contribute to the free energy of binding.[24] In contrast, SPR data is derived from much more dilute solutions than calorimetric data and it has been claimed that it includes only the direct interaction at the interface.[46,47] A comparison of thermodynamic parameters calculated from stopped flow, BIAcore and isothermal microcalorimetry on the same thrombin-inhibitor binding reaction showed significant differences. The range of values found were $+100 > \Delta H^\circ$ kJ mol$^{-1} > -100$ for enthalpy changes and $100 > \Delta S^\circ$ J mol^{-1} K$^{-1} > -100$ for entropy changes.[47]

Many workers who study carbohydrate–lectin interactions agree that they are dominated by solvation/desolvation processes of the participating solutes and that the contribution of an interaction between solute–water (as solvent) is greater than for a solute A–solute B interaction.[24,27] The hydrogen bond network of water is strong and this network is perturbed unfavourably when organic compounds are dissolved/solvated because they disrupt the normal hydrogen bonded tetrahedral structure of water. This energetically unfavourable pertubation in the structure of water derives from an unfavourable entropy term concerned with rotational entropy of water. It can be reduced or eliminated when solute A binds to solute B. A comparison of thermodynamic parameters measured in water and D_2O supported the view that a large part of the binding enthalpy change is derived from solvent reorganisation (a hydrophobic effect).[25] Enthalpy changes involve hydrogen bonding, electrostatic and van der Waals interactions that can be identified and calculated. The sources of entropy changes are much more difficult to identify and to attribute whether a contribution to the free energy of reaction will be positive or negative.

In the literature the entropic contributions have been divided into four sub-groups;[48] thus

$$\Delta S = \Delta S_{\mathrm{translational}} + \Delta S_{\mathrm{rotational}} + \Delta S_{\mathrm{vibrational}} + \Delta S_{\mathrm{conformational}}$$

The vibrational changes are claimed to be very small and for any rigid particles the conformational entropy is zero. An alternative summation of entropy changes that is more readily applied to carbohydrate–protein complex formation involves the inclusion of a solvation entropy change rather than the vibrational entropy term that is very small.[24] Thus $\Delta S = \Delta S_{T+R} + \Delta S_{solv} + \Delta S_{conf}$

The term ΔS_{T+R} is greatly reduced in water compared with the gas phase and will be further reduced in our study as the carbohydrate ligands are part of a membrane structure that will limit the translocation and rotation of the molecules mainly to two dimensions rather than three dimensions.

The freedom of rotation about the bond between thiolactose and the aglycone is greater for the C–S–C bond than a C–O–C ether bond. The thio bond is longer than the C–O bond and has a higher torsional entropy.[49] Therefore, binding of the saccharide to lectin will reduce this freedom of rotation and the translational entropy even more than any reduction that resulted from the immobilization of the ligand in the neomembrane.

In the case of the C-glycosides the saccharides are attached to the dimethylbarbituric acid *via* a quaternary carbon and one would expect the torsional entropy to be low, particularly where intramolecular hydrogen bonding can occur between the saccharide and the barbituric acid. Therefore, a major source of

negative entropy on binding has been removed and the entropic contribution to the free energy of association is positive. On binding to RCA_{120} lectin there will be a loss of conformational entropy. X-Ray studies were performed on the solid structure **20**, the tetra O-acetate of compound **14** (Fig. 6). The malonamide occupies the β-orientation at C-1 of the galactose ring, confirming the orientation derived from ^{1}H NMR coupling constants (~10 Hz).[33] The aliphatic chain (not shown) is in an extended all *trans* conformation roughly linear with the mean plane of the galactose ring and the malonamide is orthoganal to this plane. One malonamide carbonyl (O31) is hydrogen bonded to the NH (N29) of the other amide, while the other NH (N32) is hydrogen bonded to the pyranose oxygen (O52) of the galactose. It is expected that a similar situation is present in the lactosyl malonamide **15**, and that this hydrogen bonding pre-orientates or reduces the free rotation of the lactose molecule leading to a smaller loss of entropy on binding to the lectin. There maybe other plausible explanations involving the loss of steric hindrance from the larger barbiturate ring or intermolecular hydrogen bonding from the secondary amides effecting the orientation or aggregation of the C-glycolipid in the neomembrane.

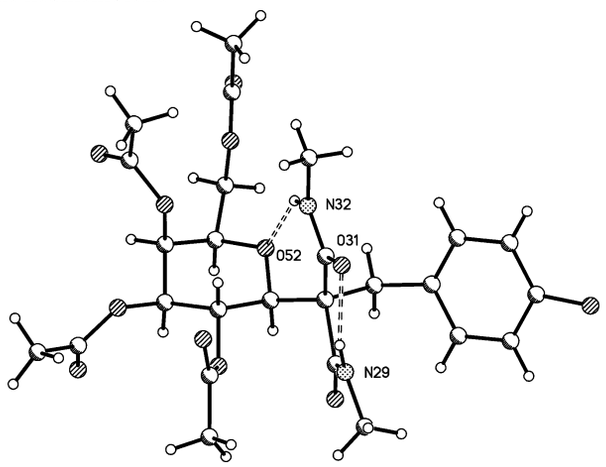

Fig. 6 The solid state stucture of compound **20**. For clarity, only the benzyloxy portion of the major component of the disordered aliphatic tail is shown. Selected interatomic distances (Å); N29 ··· O31 2.627(15), N32 ··· O52 2.640(17).

Accepting that the main contribution to the energy changes on binding of carbohydrate to lectin are derived from the hydrophobic effect then one can explain the observations made in this paper. Compounds **11**, **15** and **24** all have a low enthalpic contribution to the free energy of association ($\Delta H^\circ < \Delta G^\circ$) and they have a high positive entropic contribution ($+\Delta S^\circ$). Key hydrogen bonds and dipolar interactions are satisfied by solute–water interactions prior to association but are lost during the binding producing an unfavourable contribution to the overall free energy. To some extent the thermodynamic parameters calculated for compound **27** can be explained by similar changes. In contrast, compounds **10**, **25** and **26** all show high changes in enthalpy ($\Delta H^\circ > \Delta G^\circ$) and negative entropic contributions to the free energy of association. In the case of these molecules the interactions lost to solvent are replaced in the complex and so the net favourable free energy that derives from the desolvation of non-polar surface area drives the formation of the complex.

The K_A values for the thiolactosyl lipids, compounds **24** and **26** with two ethylene glycol groups, were lower than those with three ethylene glycol groups, compounds **25** and **27**. The former were possibly too inflexible and hydrophobic to facilitate optimum placement of the recognition epitope of the lectin. In the case of the molecules with three ethylene glycol groups one would expect a more organised and flexible helical phase in the linker region including tightly bound water.[43] An hypothesis that may explain both the kinetic values and the thermodynamic parameters calculated for the thioglycolipid series of compounds depends on the orientation of these molecules in the membrane. Long octadecyl hydrocarbon chains align with dipalmitoyl chains of the phospholipid in a largely *trans* configuration that holds the thioglycolipid molecules in a more or less vertical position with respect to the neomembrane surface.[50] Therefore, the degree of exposure of the lactose at the membrane surface and its ability to form a stable complex with the RCA_{120} lectin will depend on the length and rigidity of the ethylene glycol linker (Fig. 7(a)). The kinetic data show that three units of ethylene glycol (compound **27**) allow better complex formation ($K_A = 1.03 \times 10^7$) and more stability ($K_D = 9.73 \times 10^{-8}$) than for compound **26** that differs by only one less ethylene glycol unit ($K_A = 2.42 \times 10^6$, $K_D = 4.13 \times 10^{-7}$). In the case of compounds **24** and **25** the short dodecyl hydrocarbon chain has a less favourable interaction with the dipalmitoyl chains of the phospholipid and the dodecyl chains will have more gauche bonds so they will show less interdigitation with the phospholipid. Moreover, the thioglycolipids may phase separate from the phospholipids into islands[51,52] (Fig. 7). This will make complex formation less efficient and less stable because of unfavourable steric factors. Compound **25** has the longer more hydrophilic three-ethylene glycol linker (compared with compound **24**) that will help to lift the lactose ligand out of the membrane surface. The binding of this compound to lectin is similar to that of compound **26** that has only two ethylene glycol units but it has the octadecyl hydrocarbon chain ($K_D = 3.39 \times 10^{-7}$). It seems that the presence of an extra ethylene glycol group can counteract the lower stability of the complex caused by the shorter dodecyl hydrocarbon chain. Compound **24** has a decyl hydrocarbon chain and only two ethylene glycol

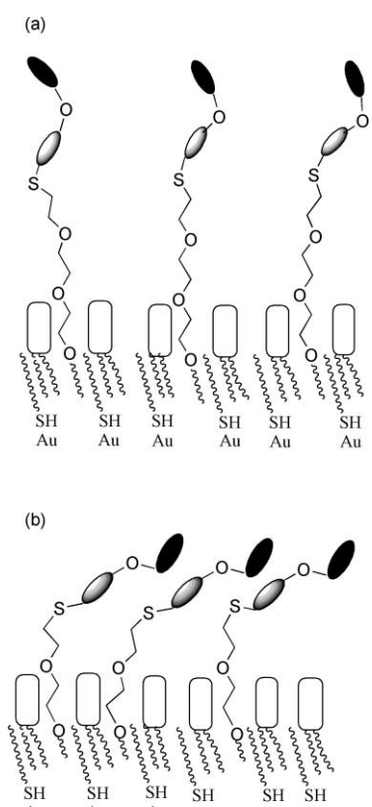

Fig. 7 The upper cartoon (a) is a diagram of compound **27** in a neomembrane of dipalmitoylphosphatidyl choline on an HPA chip surface. The octadecyl hydrocarbon chain aligned with the membrane lipids and the hydrated helix of three ethylene glycol units that project the ligand well into the aqueous domain. The dark ovals represent the galactose units, the lighter ovals represent the glucose and the clear shapes represent the zwitterionic heads of the phospholipids. The lower cartoon (b) is a diagram of compound **22** that has a shorter dodecyl hydrocarbon chain and two ethylene glycol groups. The short ethylene glycol fails to hold the ligand away from the phospholipid surface and therefore reduces binding.

units in the linker. Binding is significantly compromised (K_D = 1.16×10^{-6}) because the thiolactose ligand is too close to the membrane surface to facilitate stable complex formation. The changes in the kinetics of the reactions are reflected in the thermodynamic parameters with compound **27** having the highest $\Delta G° = -39.9$ kJ mol^{-1} of this series of compounds and compound **24** having the lowest $\Delta G° = -33.8$ kJ mol^{-1}.

The C-galactosyl lipid (compound **10**) is the exception in both series of compounds because it has only a galactosyl residue available for complex formation with RCA_{120} lectin. It has been shown that with lactosyl derivatives under favourable conditions for complex formation both the galactosyl residue and to a lesser extent the glucosyl residue are involved in binding to the RCA_{120} lectin.[52] Therefore, the maximum potential for binding the galactosyl lipid (compound **10**) will be less than the corresponding C-lactosyl lipid (compound **11**). The experiments described here show that the K_A value (2.31×10^7) for the C-lactosyl lipid was more than two orders of magnitude greater than that for the C-galactosyl lipid (8.86×10^5) and the K_D value (1.13×10^{-7} *cf.* 4.33×10^{-8}) was more than one order of magnitude greater, confirming the weaker binding of the C-galactosyl compound (**10**).

In this paper we have shown that molecules with the same lactosyl ligand and an octadecyl hydrocarbon chain have quite different affinities for RCA_{120} depending on the linker used. Moreover, the length of the hydrocarbon chain and the phospholipid environment around the chain can affect the binding of ligand to lectin at the membrane surface. These differences are reflected in the kinetics of binding and in the different values for the enthalpic and entropic contribution to the free energy of association. The importance of the linker region presenting a saccharide at the surface of a membrane should not be underestimated.

Experimental

Melting points are uncorrected. ^{1}H NMR data was recorded on a Brucker DPX-400 (400 MHz) spectrometer (δ values are in ppm using tetramethylsilane as internal standard, solvents as given). For the compounds containing disaccharides, signals for the hydrogen atoms of the sugar that are not attached directly to the barbituric acid are designated by primes, as are the second hydrogen atom of diastereotopic methylenes. ^{13}C NMR data was recorded on a Bruker DPX-400 (100 MHz). Mass spectra were recorded by the mass spectrometry service at the University of Warwick using a Waters Micromass Autospec instrument. Elemental analysis was performed by Warwick Analytical service. TLC was performed on aluminium-backed silica gel plates and visualised under UV and then charred with conc. H_2SO_4 (5%) in ethanol. All compounds were acquired from Lancaster Synthesis unless otherwise stated. RCA_{120} and dipalmitoylphosphatidylcholine were obtained from Sigma. Binding studies were monitored in real time by surface plasmon resonance using an HPA chip in a BIAcore 2000 automatic instrument. The following abbreviations were used: Ac_2O: acetic anhydride, DCM: dichloromethane, DMSO: dimethyl sulfoxide, THF: tetrahydrofuran, DMAP: 4-dimethylaminopyridine, DMF: dimethylformamide.

Crystal structure determination of *N,N′*-dimethyl-2-[2,3,4-tetra-*O*-acetyl-β-D-galactopyranosyl]-2-(4-octadecyloxybenzyl)-malonamide (16)

Crystal data. $C_{44}H_{70}N_2O_{12}$, M = 819.02, orthorhombic, a = 8.6168(8), b = 9.3641(9), c = 56.595(3) Å, U = 4566.6(7) Å^3, T = 180(2) K, space group $P2_12_12_1$ (no. 19), Z = 4, μ(Mo-Kα) = 0.086 mm^{-1}, 24773 reflections measured, 5957 unique (R_{int} = 0.065) which were used in all calculations. The final $wR(F^2)$ was 0.1276 (all data). The aliphatic tail was disordered over two positions. This disorder was traced right back to the benzene ring. The two positions were occupied in a 7 : 3 ratio and the main component was allowed to refine anisotropically.

CCDC reference number 213138.

See http://www.rsc.org/suppdata/ob/b3/b306784j/ for crystallographic data in CIF or other electronic format.

Sodium 1,3-dimethyl-5-[β-D-galactopyranosyl]barbiturate (6)[32]

Galactose (10 g, 55.5 mmol) and 1,3-dimethylbarbituric acid **5** (10 g, 64.0 mmol) were dissolved in water (120 cm^3) and $NaHCO_3$ (5.60 g) was added in small portions to moderate the effervescence. The mixture was then heated at 80 °C for 5 h and was monitored by TLC (EtOAc–MeOH–H_2O, 40 : 15 : 3 v/v) till complete conversion was achieved. The solvent was reduced to a small volume and the solution was precipitated into rapidly stirred methanol (400 cm^3). The white powdery solid was collected by filtration and recrystallized by dissolving in the minimum amount of hot water and diluting with four times the volume of methanol. On standing, large colourless hexagons of product **6** were produced (14.46 g, 82%), mp 223–224 °C; δ_H (400 MHz; D_2O) 3.20 (6H, s, NCH_3), 3.58 (1H, dd, J 3.5, 9.7, 3-H), 3.66 (3H, br s, 5-H, 6-HH^1), 3.93 (1H, d, J 3.5, 4-H), 4.40 (1H, d, J 9.7, 1-H), 4.50 (1H, t, J 9.7, 2-H); δ_C (100 MHz, D_2O) 28.1, 61.4, 67.8, 70.2, 75.5, 77.0, 79.1, 86.7, 154.7, 164.7; *m/z* 340 (M$^+$).

General procedure for the synthesis of the disaccharide barbiturate salts

The disaccharide (10 g, 29.2 mmol) and 1,3-dimethylbarbituric acid **5** (4.76 g, 30.5 mmol) were dissolved in water (120 cm^3) and $NaHCO_3$ (2.80 g) was added in small portions to moderate the effervescence. After addition the mixture was heated at 80 °C for 5 h. The solvent was reduced to a small volume and the solution was precipitated into rapidly stirred isopropanol (300 cm^3). The product was isolated by filtration and washed with a little isopropanol and diethyl ether to give the compounds below.

Sodium 1,3-dimethyl-5-[β-D-galactopyranosyl-(1 → 4)-β-D-glucopyranosyl]barbiturate (7)

Compound **7** (11.6 g, 79%) was obtained as a white powdery solid; mp 192–194 °C; δ_H (400 MHz, D_2O) 3.16 (6H, s, NCH_3), 3.60–3.48 (3H, m, 3-H, 5-H and 2′-H), 3.62 (1H, dd, J 3.3, 9.9, 3′-H), 3.74–3.66 (3H, m, 5′-H and 6′-HH′), 3.77 (1H, t, J 9.6, H-4), 3.82 (2H, d, J 2.4, 6HH′), 3.88 (1H, d, J 3.3, 4′-H), 4.35 (1H, t, J 9.8, 2-H), 4.46 (1H, d, J 7.8, 1′-H), 4.49 (1H, d, J 9.8, 1-H); δ_C (100 MHz, D_2O) 28.0, 60.5, 61.42, 69.0, 69.6, 71.4, 73.0, 75.7, 76.2, 77.1, 78.5, 78.8, 86.4, 103.3, 154.7, 165.6; *m/z* 502 (M$^+$).

Sodium 1,3-dimethyl-5-[β-D-glucopyranosyl-(1 → 4)-β-D-glucopyranosyl]barbiturate (8)

Compound **8** (12.5 g, 85%) was obtained as a white powdery solid; mp 202–204 °C; δ_H (400 MHz, D_2O) 3.16 (6H, s, NCH_3), 3.28 (1H, dd, J 8.0, 8.7, 2′-H), 3.38 (1H, t, J 9.3, 4′-H), 3.46 (2H, m, 3′-H and 5′-H), 3.52 (1H, m, 5-H), 3.57 (1H, t, J 9.5, 3-H), 3.69 (1H, dd, J 5.5, 12.1, 6′-H), 3.75 (1H, dd, J 9.5, 9.8, 4-H), 3.82 (2H, br s, 6-HH′), 3.87 (1H, br d, J 12.1, 6′-H′), 4.33 (1H, dd, J 9.5, 10.1, 2-H), 4.49 (1H, d, J 10.1, 1-H), 4.52 (1H, d, J 8.0, 1′-H); δ_C (100 MHz, D_2O) 28.0, 60.5, 61.0, 69.7, 69.9, 73.6, 75.9, 76.2, 76.4, 77.0, 78.8, 78.9, 86.4, 102.9, 154.7, 165.5; *m/z* 502 (M$^+$).

Sodium 1,3-dimethyl-5-[α-D-glucopyranosyl-(1 → 4)-β-D-glucopyranosyl]barbiturate (9)

Compound **9** (11.7 g, 80%) was obtained as a white powdery solid; mp 219–220 °C; δ_H (400 MHz, D_2O) 3.17 (6H, s, NCH_3), 3.37 (1H, t, J 9.1, 4′-H), 3.51 (1H, m, 5′-H), 3.54 (1H, dd, J 3.8,

9.9, 2′-H), 3.66 (1H, dd, *J* 9.1, 9.9, 3′-H), 3.70–3.85 (7H, m, 3-H, 4-H, 5-H, 6-HH′ and 6′-HH′), 4.34 (1H, dd, *J* 9.0, 10.0, 2-H), 4.48 (1H, d, *J* 10.0, 1-H) 5.38 (1H, d, *J* 3.8, 1′-H); δ_C (100 MHz, D_2O) 28.0, 60.9, 61.1, 67.8, 69.7, 72.3, 73.0, 73.4, 76.3, 77.5, 78.6, 79.1, 86.5, 100.2, 154.7, 165.5; *m*/*z* 502 (M^+).

4-Octadecyloxybenzaldehyde (2)[29]

4-Hydroxybenzaldehyde **1** (10 g, 81.8 mmol), 1-bromooctadecane (26 g, 80.0 mmol) and K_2CO_3 (12.6 g) were dissolved in DMF (100 cm^3). The mixture was heated at 80 °C for 24 h. The solution was precipitated into rapidly stirred water (800 ml). The solid was collected by filtration and dried. It was recrystallised from methanol to furnish a white powdery solid **2** (19.85 g, 65%); δ_H (400 MHz, $CDCl_3$) 0.86 (3H, t, *J* 6.9, $ArOCH_2CH_2CH_2(CH_2)_{14}CH_3$), 1.24 (28H, br s, $ArOCH_2CH_2CH_2(CH_2)_{14}CH_3$), 1.37 (2H, m, $ArOCH_2CH_2CH_2(CH_2)_{14}CH_3$), 1.65 (2H, qnt, *J* 6.5, $ArOCH_2CH_2CH_2(CH_2)_{14}CH_3$), 4.05 (2H, t, *J* 6.5, $ArOCH_2CH_2CH_2(CH_2)_{14}CH_3$), 7.01 (2H, d, J_{AB} 6.8, ArH), 7.85 (2H, d, J_{AB} 6.8, ArH), 9.90 (1H, s, OCH); δ_C (100 MHz, $CDCl_3$) 14.5, 23.1, 26.4, 29.5, 29.7, 29.9, 30.0, 30.1 (9 carbons unresolved under here), 32.3, 68.8, 115.2, 130.1, 132.4, 165.0, 192.0; *m*/*z* 374 (M^+)

(4-Octadecycloxyphenyl)methanol (3)[30]

4-Octadecyloxybenzaldehyde **2** (10 g, 26.70 mmol) were dissolved in methanol-THF (40 + 100 cm^3). $NaBH_4$ (1 g, 26.43 mmol) was added to the mixture in small portions. The mixture was stirred at room temperature for 1 h and was analysed by TLC (Et_2O–light petroleum (bp 60–80 °C), 1 : 4 v/v) to ensure complete conversion. The solution was precipitated into rapidly stirred ice-cold water (800 cm^3). The white precipitate was filtered off and recrystallized from methanol to give the product **3** (9.18 g, 90.9%) as needles; mp 84–85 °C (lit.[30] 84–85 °C); δ_H (400 MHz, $CDCl_3$) 0.86 (3H, t, *J* 6.9, $ArOCH_2CH_2CH_2(CH_2)_{14}CH_3$), 1.24 (28H, br s, $ArOCH_2CH_2CH_2(CH_2)_{14}CH_3$), 1.37 (2H, m, $ArOCH_2CH_2CH_2(CH_2)_{14}CH_3$), 1.65 (2H, qnt, *J* 6.5, $ArOCH_2CH_2CH_2(CH_2)_{14}CH_3$), 3.98 (2H, t, *J* 6.5, $ArOCH_2CH_2(CH_2)_{15}CH_3$), 4.63 (2H, s, $ArCH_2OH$), 6.92 (2H, d, J_{AB} 6.8, ArH), 7.30 (2H, d, J_{AB} 6.8, ArH); δ_C (100 MHz, $CDCl_3$) 14.5, 23.1, 26.5, 29.7(3), 29.7(7), 29.8, 29.9, 30.0(1), 30.0(7), 30.2 (7 carbons unresolved under here), 32.3, 65.5, 68.5, 115.0, 129.0, 133.0, 158.2; *m*/*z* 376 (M^+).

1-Chloromethyl-4-octadecyloxybenzene (4)

(4-Octadecycloxyphenyl)methanol **3** (1.25 g, 3.32 mmol) was dissolved in DCM (20 cm^3) and to this was added $SOCl_2$ (0.5 cm^3, 6.8 mmol). The reaction mixture was stirred at room temperature for 24 h and was analysed by TLC (DCM) to ensure complete conversion. The solvent was removed at reduced pressure to furnish a white powder. The solid was recrystallized from acetonitrile to furnish **4** (1.1 g, 84%) as white needles and used without further purification, δ_H (400 MHz, $CDCl_3$) 0.86 (3H, t, *J* 6.9, $ArOCH_2CH_2CH_2(CH_2)_{14}CH_3$), 1.24 (28H, br s, $ArOCH_2CH_2CH_2(CH_2)_{14}CH_3$), 1.37 (2H, m, $ArOCH_2CH_2CH_2(CH_2)_{14}CH_3$), 1.65 (2H, p, *J* 6.5, $ArOCH_2CH_2CH_2(CH_2)_{14}CH_3$), 3.98 (2H, t, *J* 6.5, $ArOCH_2CH_2(CH_2)_{15}CH_3$), 4.61 (2H, s, $ArCH_2Cl$), 6.90 (2H, d, J_{AB} 6.8, ArH), 7.32 (2H, d J_{AB} 6.8, ArH); δ_C (100 MHz, $CDCl_3$) 14.5, 23.1, 26.4, 29.6, 29.8, 29.9, 30.0, 30.1 (9 carbons unresolved under here), 32.3, 46.8, 68.5, 115.1, 130.0, 130.4, 160.0; *m*/*z* 394/396 (M^+).

1,3-Dimethyl-5-[β-D-galactopyranosyl]-5-(4-octadecyloxybenzyl)pyrimidine-2,4,6-trione (10)

Galactose barbituric salt **6** (1 g, 2.94 mmol) and 1-chloromethyl-4-octadecyloxybenzene **4** (1 g, 2.55 mmol) were dissolved in DMSO (20 cm^3) and the reaction mixture was heated and stirred at 70 °C for 3 h. After this time the reaction mixture was analysed by TLC (EtOAc–MeOH–H_2O, 20 : 20 : 4 v/v) to ensure complete conversion. The DMSO was then removed under high vacuum and the solid mixture tritriated with water to remove salts. The solid was placed on a column of silica and eluted with EtOAc then with EtOAc containing an increasing concentration (0–20%) of MeOH–water (5 : 1 v/v). Evaporation of the fractions that contained product under reduced pressure gave a white powder that was recrystallised from EtOAc to give **10** (0.98 g, 57%) as tiny needles; mp 144–147 °C; δ_H (400 MHz, d_6-DMSO) 0.86 (3H, t, *J* 6.9, $ArOCH_2CH_2(CH_2)_{15}CH_3$), 1.24 (28H, br s, $ArOCH_2CH_2CH_2(CH_2)_{14}CH_3$), 1.37 (2H, m, $ArOCH_2CH_2CH_2(CH_2)_{14}CH_3$), 1.65 (2H, qnt, *J* 6.5, $ArOCH_2CH_2CH_2(CH_2)_{14}CH_3$), 2.95 (3H, s, NCH_3), 3.00 (3H, s, NCH_3), 3.25–3.37 (4H, m, 3-H, 5-H, CHH^1Ar), 3.46 (2H, m, $C6HH^1$), 3.58 (1H, ddd, *J* 5.9, 9.1, 9.6, 2-H), 3.66 (1H, br t, *J* 3.9, 4-H), 3.75 (1H, d, *J* 9.6, 1-H), 3.86 (2H, t, *J* 6.5, $ArOCH_2CH_2CH_2(CH_2)_{14}CH_3$), 4.28 (1H, d, *J* 3.9, 4-OH), 4.52 (1H, t, *J* 5.6, 6-OH), 4.70 (1H, d, *J* 6.0, 3-OH), 5.50 (1H, d, *J* 5.9, 2-OH), 6.78 (2H, d, J_{AB} 8.7, ArH), 6.82 (2H, d, J_{AB} 8.7, ArH); δ_C (100 MHz, d_6-DMSO) 14.3, 22.5, 25.9, 28.2, 28.3, 29.0, 29.1, 29.2, 29.4 (10 carbons unresolved under here), 31.7, 40.0, 60.7, 60.8, 67.6, 68.6, 68.7, 75.4, 80.4, 83.7, 114.5, 127.2, 130.5, 150.8, 158.0, 170.0, 170.1; *m*/*z* 699 ($M + Na^+$).

1,3-Dimethyl-5-[β-D-galactopyranosyl-(1 ⟶ 4)-β-D-glucopyranosyl]-5-(4-octadecyloxybenzyl)pyrimidine-2,4,6-trione (11)

Lactose barbituric salt **7** (1 g, 1.99 mmol) and 1-chloromethyl-4-octadecyloxybenzene **4** (1 g, 2.58 mmol) were dissolved in DMSO (20 cm^3) and the reaction mixture was heated and stirred at 70 °C for 3 h. The reaction mixture was analysed by TLC (EtOAc–MeOH–H_2O, 40 : 20 : 4 v/v) to ensure complete conversion. The DMSO was then removed under high vacuum and the solid was dissolved in boiling water (20 cm^3) and allowed to cool. The solid was filtered off and air dried then placed on a column of silica and eluted with EtOAc, then with EtOAc containing an increasing concentration (0–20%) of MeOH–water (5 : 1 v/v). Evaporation of the fractions that contained product under reduced pressure gave a white powder that was recrystallized from acetone as a white powdery product **11** (0.91 g, 55%); mp 143–145 °C;. δ_H (400 MHz, d_6-DMSO) 0.86 (3H, t, *J* 6.9, $ArOCH_2CH_2CH_2(CH_2)_{14}CH_3$), 1.25 (28H, br s, $ArOCH_2CH_2CH_2(CH_2)_{14}CH_3$), 1.37 (2H, m, $ArOCH_2CH_2CH_2(CH_2)_{14}CH_3$), 1.66 (2H, qnt, *J* 6.9, $ArOCH_2CH_2CH_2(CH_2)_{14}CH_3$), 2.94 (3H, s, NCH_3), 3.00 (3H, s, NCH_3), 3.20 (2H, m, 5′-H, $CHH'Ar$), 3.24–3.34 (6H, m, 2-H, 3-H, 4-H, 5-H, 2′-H and 3′-H), 3.45–3.55 (3H, m, 6-H, 6′-HH′), 3.45 (1H, d, J_{AB} 13.4, $CHH'Ar$), 3.63 (1H, br s, 4′-H), 3.79 (1H, m, 6-H′), 3.87 (3H, m, 1-H, $ArOCH_2CH_2CH_2(CH_2)_{14}CH_3$), 4.21 (1H, d, *J* 7.2, 1′-H), 4.53 (2H, br s, OH), 4.64 (1H, br s, OH), 4.74 (1H, br s, OH), 4.79 (1H, br s, OH), 5.12 (1H, br s, OH), 5.49 (1H, br d, *J* 5.5, 2-OH), 6.77 (2H, d, J_{AB} 8.9, ArH), 6.81 (2H, d, J_{AB} 8.9, ArH); δ_C (100 MHz, d_6-DMSO) 14.3, 22.5, 25.8, 28.2, 28.3, 29.0, 29.1, 29.1, 29.3(4), 29.3(6), 29.3(7) (8 carbons unresolved under here), 29.4, 31.7, 40.6, 60.2, 60.8, 61.1, 67.7, 68.5, 70.9, 71.6, 73.6, 75.9, 76.7, 80.3, 81.1, 82.4, 104.1, 114.6, 126.8, 130.4, 150.6, 158.1, 169.8, 170.1; *m*/*z* 861 ($M + Na^+$)

1,3-Dimethyl-5-[β-D-glucopyranosyl-(1 ⟶ 4)-β-D-glucopyranosyl]-5-(4-octadecyloxybenzyl)pyrimidine-2,4,6-trione (12)

The same procedure was followed as for the alkylation of sodium 1,3-dimethyl-5-[β-D-galactopyranosyl-(1 ⟶ 4)-β-D-glucopyranosyl]barbiturate **11** above. Evaporation of the fractions that contained product under reduced pressure gave a white powder that was recrystallized from ethyl acetate as a white powdery product **12** (1.13 g, 68%); mp 146–149 °C from EtOAc. δ_H (400 MHz, d_6-DMSO) 0.86 (3H, t, *J* 6.9, $ArOCH_2CH_2CH_2(CH_2)_{14}CH_3$), 1.25 (28H, br s, $ArOCH_2CH_2CH_2(CH_2)_{14}CH_3$), 1.37 (2H, m, $ArOCH_2CH_2CH_2(CH_2)_{14}CH_3$), 1.66 (2H, qnt,

J 6.9, ArOCH$_2$C*H*$_2$CH$_2$(CH$_2$)$_{14}$CH$_3$), 2.95 (3H, s, NCH$_3$), 3.00 (3H, s, NCH$_3$), 2.95–3.10 (2H, m, 2′-H and 3′-H), 3.15–3.45 (9H, m, 2-H, 3-H, 4-H, 5-H, 4′-H, 5′-H, 6′-H, CHH′Ar), 3.55 (1H, m, 6-H), 3.75 (2H, m, 6-H′, 6′-H′), 3.87 (3H, m, 1-H, ArOC*H*$_2$CH$_2$CH$_2$(CH$_2$)$_{14}$CH$_3$), 4.26 (1H, d, J 7.9, 1′-H), 4.56 (1H, br t, *J* 5.9, 6′-OH), 4.58 (1H, br t, *J* 5.2, 6-OH), 4.70 (1H, br s, 4′-OH), 5.00 (1H, br d, *J* 4.8, 3-OH), 5.03 (1H, br d, *J* 4.8, 3′-OH), 5.26 (1H, br d, *J* 4.8, 2′-OH), 5.49 (1H, br d, *J* 5.7, 2-OH), 6.77 (2H, d, J_{AB} 8.6, ArH), 6.81 (2H, d, J_{AB} 8.6, ArH); δ_C (100 MHz, d$_6$-DMSO) 14.3, 22.5, 25.9, 28.2, 28.3, 29.0, 29.1, 29.3(4), 29.3(5), 29.3(6) (8 carbons unresolved under here), 29.4, 31.7, 40.6, 60.2, 61.0, 61.4, 67.6, 70.4, 71.5, 73.6, 76.8, 76.9, 77.1, 80.3, 80.9, 82.4, 103.5, 114.6, 126.8, 130.4, 150.6, 158.1, 169.9, 170.1; *m*/*z* (M + Na$^+$) 862

1,3-Dimethyl-5-[α-D-glucopyranosyl-(1 ⟶ 4)-β-D-glucopyranosyl]-5-(4-octadecyloxybenzyl)pyrimidine-2,4,6-trione (13)

The same procedure was followed as for the alkylation of sodium 1,3-dimethyl-5-[β-D-galactopyranosyl-(1 ⟶ 4)-β-D-glucopyranosyl]barbiturate **11** above. Evaporation of the fractions that contained product under reduced pressure gave a white powder that was recrystallised from acetone as a white powdery product **13** (0.98 g, 59%); mp 142–144 °C from EtOAc;. δ_H (400 MHz, d$_6$-DMSO) 0.86 (3H, t, *J* 6.9, ArOCH$_2$CH$_2$CH$_2$(CH$_2$)$_{14}$-C*H*$_3$), 1.25 (28H, br s, ArOCH$_2$CH$_2$CH$_2$(C*H*$_2$)$_{14}$CH$_3$) 1.37 (2H, m, ArOCH$_2$CH$_2$C*H*$_2$(CH$_2$)$_{14}$CH$_3$), 1.66 (2H, qnt, *J* 6.9, ArO-CH$_2$C*H*$_2$CH$_2$(CH$_2$)$_{14}$CH$_3$), 2.95 (3H, s, NCH$_3$), 2.99 (3H, s, NCH$_3$), 3.08 (1H, m, 4′-H), 3.15–3.55 (11H, m, 2-H, 3-H, 4-H, 5-H, 6-H, 2′-H, 3′-H, 5′-H, 6′-H, CHH′Ar), 3.63 (1H, m, 6-H′), 3.71 (1H, dd, *J* 5.3, 11.5, 6′-H′), 3.87 (3H, m, 1-H, ArOC*H*$_2$CH$_2$CH$_2$(CH$_2$)$_{14}$CH$_3$), 4.45 (1H, t, *J* 5.6, 6-OH), 4.54 (1H, t, *J* 5.6, 6′-OH), 4.90 (2H, m, 2 × OH), 5.00 (1H, d, *J* 3.2, 1′-H), 5.42 (1H, d, *J* 5.5, OH), 5.52 (2H, m, 2 × OH), 6.77 (2H, d, J_{AB} 8.6, ArH), 6.81 (2H, d, J_{AB} 8.6, ArH); δ_C (100 MHz, d$_6$-DMSO) 14.3, 22.5, 25.8, 28.2, 28.3, 28.9, 29.0, 29.1, 29.4 (10 carbons unresolved under here), 31.5, 40.1, 60.3, 61.1, 61.3, 67.6, 70.2, 71.2, 72.7, 73.6, 73.8, 78.5, 80.2, 80.6, 82.8, 101.2, 114.6, 126.8, 130.4, 150.6, 158.1, 169.9, 170.1; *m*/*z* 862 (M + Na$^+$).

N,N′-Dimethyl-2-[β-D-galactopyranosyl]-2-(4-octadecyloxybenzyl)malonamide (14)

1,3-Dimethyl-5-[β-D-galactopyranosyl]-5-(4-octadecyloxybenzyl)pyrimidine-2,4,6-trione **10** (0.5 g, 0.74 mmol) was dissolved in THF (10 cm^3) and 1 M NaOH (2 cm^3, excess) was added dropwise over 5 min to the stirred solution. The reaction mixture was stirred at room temperature for 2 h until the starting material was consumed (TLC: EtOAc–MeOH–H$_2$O, 40 : 5 : 1 v/v). The reaction mixture was neutralised with 1 M HCl. Water (20 cm^3) was added and the THF was removed at reduced pressure. The solution was chilled in ice and the resulting solid collected by filtration and dried. The solid was recrystallised from ethyl acetate to furnish a white powder **14** (0.39 g, 81%); δ_H (400 MHz, d$_6$-DMSO) 0.86 (3H, t, *J* 6.7, ArOCH$_2$CH$_2$CH$_2$(CH$_2$)$_{14}$-C*H*$_3$), 1.25 (28H, br s, ArOCH$_2$CH$_2$CH$_2$(C*H*$_2$)$_{14}$CH$_3$), 1.39 (2H, m, ArOCH$_2$CH$_2$C*H*$_2$(CH$_2$)$_{14}$CH$_3$), 1.67 (2H, qnt, *J* 6.4, ArOCH$_2$C*H*$_2$CH$_2$(CH$_2$)$_{14}$CH$_3$), 2.50 (3H, d, *J* 4.5, NHC*H*$_3$), 2.63 (3H, d, *J* 4.5, NHC*H*$_3$), 3.11 (1H, d, J_{AB} 13.4, C*H*H′Ar), 3.26 (1H, d, J_{AB} 13.4, CH*H*′Ar), 3.28 (1H, dd, *J* 2.8, 8.90, 3-H), 3.40 (2H, m, 2-H, 5-H), 3.56 (1H, dd, *J* 5.1, 11.3, 6-H), 3.63 (1H, dd, *J* 6.9, 11.3, 6-H′), 3.70 (1H, d, *J* 2.8, 4-H), 3.83 (1H, d, *J* 9.6, 1-H), 3.88 (2H, t, *J* 6.4, ArOC*H*$_2$CH$_2$CH$_2$(CH$_2$)$_{14}$-CH$_3$), 4.25 (4H, br s, 4 × OH), 6.72 (2H, d, J_{AB} 8.6, ArH), 6.94 (2H, d, J_{AB} 8.6, ArH), 7.67 (1H, q, *J* 4.5, N*H*CH$_3$), 8.88 (1H, q, *J* 4.5, N*H*CH$_3$); δ_C (100MHz, d$_6$-DMSO) 14.3, 22.5, 25.9, 26.0, 26.2, 29.1(0), 29.1(5), 29.2, 29.3 (9 carbons unresolved under here), 29.4, 31.7, 39.9, 59.9, 61.3, 67.5, 68.8, 69.4, 75.4, 79.7, 81.1, 113.8, 129.3, 131.0, 157.6, 171.0, 172.8; *m*/*z* 651 (M + H$^+$).

N,N′-Dimethyl-2-[β-D-galactopyranosyl-(1 ⟶ 4)-β-D-glucopyranosyl]-2-(4-octadecyloxybenzyl)malonamide (15)

1,3-Dimethyl-5-[β-D-galactopyranosyl-(1 ⟶ 4) -β-D-glucopyranosyl]-5-(4-octadecyloxybenzyl)pyrimidine-2,4,6-trione **11** (0.5 g, 0.59 mmol) was dissolved in THF (10 cm^3) and 1 M NaOH (2 cm^3, excess) was added dropwise over 5 min to the stirred solution. The reaction mixture was stirred at room temperature for 1 h until the starting material was consumed (TLC: EtOAc–MeOH–H$_2$O, 40 : 10 : 2 v/v). The reaction mixture was neutralised with 1 M HCl. Water (20 cm^3) was added and the THF was removed under reduced pressure. The solution was chilled in ice and the resulting solid was collected by filtration and dried to give the product **15** as a powder (0.25 g, 52%); mp 210–211 °C; δ_H (400 MHz, d$_6$-DMSO) 0.86 (3H, t, *J* 6.9, ArO-CH$_2$CH$_2$CH$_2$(CH$_2$)$_{14}$C*H*$_3$), 1.24 (28H, br s, ArOCH$_2$CH$_2$CH$_2$-(C*H*$_2$)$_{14}$CH$_3$), 1.38 (2H, m, ArOCH$_2$CH$_2$C*H*$_2$(CH$_2$)$_{14}$CH$_3$), 1.67 (2H, qnt, *J* 6.9, ArOCH$_2$C*H*$_2$CH$_2$(CH$_2$)$_{14}$CH$_3$), 2.49 (3H, d, *J* 4.5, NHC*H*$_3$), 2.65 (3H, d, *J* 4.5, NHC*H*$_3$), 3.02 (1H, t, *J* 9.1, 2-H), 3.10 (1H, d, J_{AB} 13.5, C*H*H′Ar), 3.20–3.40 (6H, m, 3-H, 4-H, 2′-H, 3′-H, 5′-H, CH*H*′Ar), 3.51–3.60 (3H, m, 4-H, 6′-HH′), 3.64 (1H, br s, 4′-H), 3.76 (2H, m, 6-HH′), 3.87 (3H, m, 1-H, ArOC*H*$_2$CH$_2$CH$_2$(CH$_2$)$_{14}$CH$_3$), 4.19 (1H, d, *J* 6.5, 1′-H), 4.71 (7H, br s, 7 × OH), 6.72 (2H, d, J_{AB} 8.5, ArH), 6.93 (2H, d, J_{AB} 8.5, ArH), 7.65 (1H, q, *J* 4.5, N*H*CH$_3$), 9.00 (1H, q, *J* 4.5, N*H*CH$_3$); δ_C (100MHz, d$_6$-DMSO) 14.3, 22.5, 25.9, 26.0, 26.3, 29.1(0), 29.1(5), 29.3(5), 29.3(7) (9 carbons unresolved under here), 29.4, 31.7, 39.9, 59.6, 59.9, 60.7, 67.5, 68.5, 70.9, 72.3, 73.6, 75.8, 76.6, 79.4, 79.9, 80.4, 104.2, 113.8, 129.1, 130.9, 157.6, 170.9, 172.1; *m*/*z* 835 (M + Na$^+$).

General procedure for the acetylations

The sugar derivative (0.5 g), acetic anhydride (5 cm^3) and a catalytic amount of DMAP (50 mg) were dissolved in pyridine (5 cm^3). The reaction mixture was stirred at room temperature for 24 h. Water (20 cm^3) was added to the reaction mixture and it was stirred for 30 min. The mixture was extracted with DCM (3 × 20 cm^3). The combined DCM fractions were washed with saturated NaHCO$_3$ (2 × 25 cm^3) followed by 1 M HCl (2 × 25 cm^3). The combined DCM fractions were dried with MgSO$_4$, filtered and the solvent removed under reduced pressure to give the required compounds.

1,3-Dimethyl-5-[2,3,4,6-tetra-*O*-acetyl-β-D-galactopyranosyl]-5-(4-octadecyloxybenzyl)pyrimidine-2,4,6-trione (16)

Compound **16** (0.52 g, 83%); δ_H (400 MHz, CDCl$_3$) 0.81 (3H, t, *J* 6.7, ArOCH$_2$CH$_2$CH$_2$(CH$_2$)$_{14}$C*H*$_3$), 1.19 (28H, br s, ArO-CH$_2$CH$_2$CH$_2$(C*H*$_2$)$_{14}$CH$_3$),1.35(2H,m,ArOCH$_2$CH$_2$C*H*$_2$(CH$_2$)$_{14}$-CH$_3$), 1.67 (2H, qnt, *J* 6.8, ArOCH$_2$C*H*$_2$CH$_2$(CH$_2$)$_{14}$CH$_3$), 1.90 (6H, s, 2 × OCOCH$_3$), 1.94 (3H, s, OCOCH$_3$), 2.10 (3H, s, OCOCH$_3$), 3.00 (3H, s, NCH$_3$), 3.07 (3H, s, NCH$_3$), 3.09 (1H, d, J_{AB} 12.9, C*H*H′Ar), 3.27 (1H, d, J_{AB} 12.9, CH*H*′Ar), 3.80 (3H, m, 5-H, ArOC*H*$_2$CH$_2$CH$_2$(CH$_2$)$_{14}$CH$_3$), 3.97 (2H, m, 6-HH′), 4.29 (1H, d, *J* 9.9, 1-H), 4.96 (1H, dd, *J* 3.0, 9.7, 3-H), 5.30 (1H, d, *J* 3.0, 4-H), 5.67 (1H, dd, *J* 9.7, 9.9, 2-H), 6.64 (2H, d, J_{AB} 8.3, ArH), 6.80 (2H, d, J_{AB} 8.3, ArH); δ_C (100 MHz, CDCl$_3$) 14.5, 20.9 (2 carbons unresolved under here), 21.0(4), 21.0(7), 23.0, 26.4, 28.6, 28.7, 29.6, 29.7, 29.8, 29.9, 30.0 (9 carbons unresolved under here), 32.3, 40.7, 60.9, 61.9, 67.5, 67.8, 68.3, 73.3, 75.3, 81.2, 114.8, 125.6, 130.7, 150.5, 159.2, 169.2, 169.4, 169.9, 170.4, 170.5, 170.6; *m*/*z* 845 (M + H$^+$). Found: C, 63.81, H, 8.10, N, 3.23%. $C_{45}H_{68}N_2O_{13}$ requires C, 63.96, H, 8.11, N, 3.32%.

1,3-Dimethyl-5-[2,3,4,6-tetra-*O*-acetyl-β-D-galactopyranosyl-(1 ⟶ 4)-2,3,6-tri-*O*-acetyl-β-D-glucopyranosyl]-5-(4-octadecyloxybenzyl)pyrimidine-2,4,6-trione (17)

Compound **17** (0.56 g, 83%); δ_H (400 MHz, CDCl$_3$) 0.85 (3H, t, *J* 6.7, ArOCH$_2$CH$_2$CH$_2$(CH$_2$)$_{14}$C*H*$_3$), 1.22 (28H, br s, ArO-

$CH_2CH_2CH_2(CH_2)_{14}CH_3$), 1.39 (2H, m, $ArOCH_2CH_2CH_2$-$(CH_2)_{14}CH_3$), 1.70 (2H, qnt, *J* 6.8, $ArOCH_2CH_2CH_2(CH_2)_{14}$-$CH_3$), 1.93 (3H, s, $OCOCH_3$), 1.96 (3H, s, $OCOCH_3$), 1.99 (3H, s, $OCOCH_3$), 2.00 (3H, s, $OCOCH_3$), 2.01 (3H, s, $OCOCH_3$), 2.05 (3H, s, $OCOCH_3$), 2.12 (3H, s, $OCOCH_3$), 3.02 (3H, s, NCH_3), 3.04 (1H, d, J_{AB} 12.8, CHH′Ar), 3.10 (3H, s, NCH_3), 3.23 (1H, d, J_{AB} 12.8, CHH′Ar), 3.50 (1H, m, 5-H), 3.69 (1H, t, *J* 9.4, 4-H), 3.83 (3H, m, 5′-H, $ArOCH_2CH_2CH_2(CH_2)_{14}CH_3$), 3.91 (1H, dd, *J* 5.2, 12.0, 6-H), 4.08 (2H, m, 6′-HH′), 4.30 (1H, d, *J* 10.0, 1-H), 4.46 (1H, d, *J* 7.9, 1′-H), 4.48 (1H, dd, *J* 2.0, 12.0, 6-H′), 4.93 (1H, dd, *J* 3.4, 10.4, 3′-H), 5.07 (1H, dd, *J* 7.9, 10.4, 2′-H), 5.14 (1H, t, *J* 9.4, 3-H), 5.31 (1H, d, *J* 3.4, 4′-H), 5.52 (1H, dd, *J* 9.4, 10.0, 2-H), 6.66 (2H, d, J_{AB} 8.6, ArH), 6.81 (2H, d, J_{AB} 8.6, ArH); δ_C (100 MHz, $CDCl_3$) 14.5, 20.8, 20.9, 21.0 (2 carbons unresolved under here), 21.1(0), 21.1(5), 21.2, 23.1, 26.4, 28.6(5), 28.6(8), 29.6, 29.7, 29.8, 29.9(5), 29.9(8), 30.1 (8 carbons unresolved under here), 32.3, 40.4, 61.1, 61.2, 61.6, 67.0, 68.4, 69.5, 70.3, 71.1, 71.3, 75.2, 76.2, 77.5, 80.7, 101.4, 114.9, 125.6, 130.7, 150.5, 159.2, 169.4, 169.5, 169.6, 170.0, 170.3, 170.4(1), 170.4(6), 170.5, 170.75; *m*/*z* 1133 (M^+). Found: C, 60.71, H, 7.59, N, 2.41%. $C_{57}H_{84}N_2O_{21}$ requires C, 60.41, H, 7.47, N, 2.47%.

1,3-Dimethyl-5-[2,3,4,6-tetra-*O*-acetyl-β-D-glucopyranosyl-(1 → 4)-2,3,6-tri-*O*-acetyl-β-D-glucopyranosyl]-5-(4-octadecyloxybenzyl)pyrimidine-2,4,6-trione (18)

Compound **18** (0.59 g, 87%); δ_H (400 MHz, $CDCl_3$) 0.90 (3H, t, *J* 6.9, $ArOCH_2CH_2CH_2(CH_2)_{14}CH_3$), 1.28 (28H, br s, ArO-$CH_2CH_2CH_2(CH_2)_{14}CH_3$),1.45(2H,m,$ArOCH_2CH_2CH_2(CH_2)_{14}$-$CH_3$), 1.76 (2H, qnt, *J* 6.5, $ArOCH_2CH_2CH_2(CH_2)_{14}CH_3$), 2.00 (3H, s, $OCOCH_3$), 2.01 (3H, s, $OCOCH_3$), 2.03 (3H, s, $OCOCH_3$), 2.04 (6H, s, 2 × $OCOCH_3$), 2.05 (3H, s, $OCOCH_3$), 2.13 (3H, s, $OCOCH_3$), 3.10 (3H, s, NCH_3), 3.13 (1H, d, J_{AB} 12.9, CHH′Ar), 3.15 (3H, s, NCH_3), 3.28 (1H, J_{AB} 12.9, CHH′Ar), 3.54 (1H, m, 5-H), 3.68 (1H, m, 5′-H), 3.73 (1H, t, *J* 9.4, 4-H), 3.88 (2H, t, *J* 6.5, $ArOCH_2CH_2CH_2(CH_2)_{14}CH_3$), 3.96 (1H, dd, *J* 5.1, 12.0, 6-H), 4.07 (1H, dd, *J* 1.8, 12.5, 6′-H), 4.34 (1H, d, *J* 9.9, 1-H), 4.40 (1H, dd, *J* 4.4, 12.5, 6′-H′), 4.52 (1H, d, *J* 7.9, 1′-H), 4.56 (1H, d, *J* 12.0, 6-H′), 4.95 (1H, dd, *J* 7.9, 9.1, 2′-H), 5.09 (1H, t, *J* 9.5, 4′-H), 5.17 (2H, br t, *J* ~9.1, 3-H, 3′-H), 5.59 (1H, dd, *J* 9.1, 9.9, 2-H), 6.71 (2H, d, J_{AB} 8.6, ArH), 6.87 (2H, d, J_{AB} 8.6, ArH); δ_C (100 MHz, $CDCl_3$) 14.5, 20.9 (3 carbons unresolved under here), 21.0(3), 21.0(7), 21.2, 23.1, 26.4, 28.7 (2 carbons unresolved under here), 29.6, 29.7, 29.8, 30.0, 30.1 (10 carbons unresolved under here), 32.3, 40.4, 61.0, 61.5, 61.9, 68.1, 68.4, 70.2, 72.0, 72.4, 73.3, 74.9, 76.4, 77.6, 80.8, 101.2, 114.9, 125.5, 130.7, 150.5, 159.2, 169.3, 169.5 (2 carbons unresolved under here), 169.7, 170.0, 170.3, 170.4, 170.6, 170.9; *m*/*z* 1133 (M + H^+). Found: C, 60.54, H, 7.49, N, 2.44%. $C_{57}H_{84}N_2O_{21}$ requires C, 60.41, H, 7.47, N, 2.47%.

1,3-Dimethyl-5-[2,3,4,6-tetra-*O*-acetyl-α-D-glucopyranosyl-(1 → 4)-2,3,6-tri-*O*-acetyl-β-D-glucopyranosyl]-5-(4-octadecyloxybenzyl)pyrimidine-2,4,6-trione (19)

Compound **19** (0.55 g, 82%), δ_H (400 MHz, $CDCl_3$) 0.81 (3H, t, *J* 6.8, $ArOCH_2CH_2CH_2(CH_2)_{14}CH_3$), 1.18 (28H, m, $ArOCH_2$-$CH_2CH_2(CH_2)_{14}CH_3$), 1.35 (2H, m, $ArOCH_2CH_2CH_2(CH_2)_{14}$-$CH_3$), 1.66 (2H, qnt, *J* 6.6, $ArOCH_2CH_2CH_2(CH_2)_{14}CH_3$), 1.90 (3H, s, $OCOCH_3$), 1.93 (3H, s, $OCOCH_3$), 1.94 (3H, s, $OCOCH_3$), 1.95 (3H, s, $OCOCH_3$), 1.97 (3H, s, $OCOCH_3$), 1.98 (3H, s, $OCOCH_3$), 2.02 (3H, s, $OCOCH_3$), 3.01 (3H, s, NCH_3), 3.03 (1H, d, J_{AB} 12.8, CHH′Ar), 3.05 (3H, s, NCH_3), 3.18 (1H, d, J_{AB} 12.8, CHH′Ar), 3.53 (1H, m, 5-H), 3.78 (2H, t, *J* 6.6, $ArOCH_2CH_2CH_2(CH_2)_{14}CH_3$), 3.83 (1H, t, *J* 8.8, 4-H), 3.88 (1H, m, 5′-H), 3.95 (1H, dd, *J* 4.6, 12.2, 6-H), 3.98 (1H, dd, *J* 2.0, 12.4, 6′-H), 4.18 (1H, dd, *J* 3.8, 12.4, 6′-H′), 4.33 (1H, d, *J* 9.8, 1-H), 4.47 (1H, dd, *J* 2.3, 12.2, 6-H′), 4.79 (IH, dd, *J* 4.0, 10.5, 2′-H), 4.97 (1H, t, *J* 9.4, 4′-H), 5.19 (1H, t, *J* 8.8, 3-H), 5.27 (1H, dd, *J* 9.4, 10.5, 3′-H), 5.32 (1H, d, *J* 4.0, 1′-H), 5.45 (1H, dd, *J* 8.8, 9.8, 2-H), 6.62 (2H, d, J_{AB} 8.6, ArH), 6.78 (2H, d, J_{AB} 8.6, ArH); δ_C (100 MHz, $CDCl_3$) 14.5, 20.9 (3), 20.9 (9), 21.0, 21.1, 21.4, 23.1, 26.4, 28.6(4), 28.6(8), 29.6, 29.7(1), 29.7(7), 29.9(3), 29.9(5), 30.1 (10 carbons unresolved under here), 32.3, 40.3, 61.1, 61.8, 62.3, 68.3, 68.4, 68.9, 69.7, 70.4, 70.7, 72.7, 77.0, 77.7, 80.6, 96.1, 114.9, 125.5, 130.7, 150.5, 159.2, 169.5, 169.6, 169.7, 170.0, 170.2, 170.3, 170.8 (2 carbons unresolved under here), 170.9; *m*/*z* 1156 (M + Na^+). Found: C, 60.44, H, 7.39, N, 2.41%, $C_{57}H_{84}N_2O_{21}$ requires C, 60.41, H, 7.47, N, 2.47%.

N,N′-Dimethyl-2-[2,3,4,6-tetra-*O*-acetyl-β-D-galactopyranosyl]-2-(4-octadecyloxybenzyl)malonamide (20)

Compound **20** (0.49 g, 78%); mp 137–138 °C (from Et_2O–light petroleum (bp 60–80 °C)); δ_H (400 MHz, $CDCl_3$) 0.80 (3H, t, *J* 6.7, $ArOCH_2CH_2CH_2(CH_2)_{14}CH_3$), 1.18 (28H, br s, $ArOCH_2$-$CH_2CH_2(CH_2)_{14}CH_3$), 1.36 (2H, m, $ArOCH_2CH_2CH_2(CH_2)_{14}$-$CH_3$), 1.67 (2H, qnt, *J* 6.7, $ArOCH_2CH_2CH_2(CH_2)_{14}CH_3$), 1.81 (3H, s, $OCOCH_3$), 1.87 (3H, s, $OCOCH_3$), 2.00 (3H, s, $OCOCH_3$), 2.10 (3H, s, $OCOCH_3$), 2.52 (3H, d, *J* 4.7, $NHCH_3$), 2.85 (3H, d, *J* 4.6, $NHCH_3$), 3.02 (1H, d, J_{AB} 13.3, CHH′Ar), 3.14 (1H, d, J_{AB} 13.3, CHH′Ar), 3.82 (2H, t, *J* 6.7, $ArOCH_2$-$CH_2CH_2(CH_2)_{14}CH_3$), 3.95 (1H, dd, *J* 4.9, 11.1, 6-H), 4.01 (1H, dd, *J* 4.9, 7.5, 5-H), 4.39 (1H, dd, *J* 7.5, 11.1, 6-H′), 4.59 (1H, d, *J* 10.2, 1-H), 4.97 (1H, dd, *J* 3.0, 9.9, 3-H), 5.24 (1H, dd, *J* 9.9, 10.2, 2-H), 5.40 (1H, d, *J* 3.0, 4-H), 6.66 (2H, d, J_{AB} 8.6, ArH), 6.83 (2H, d, J_{AB} 8.6, ArH), 7.20 (1H, q, *J* 4.6, $NHCH_3$), 9.23 (1H, q, *J* 4.7, $NHCH_3$); δ_C (100 MHz, $CDCl_3$) 13.1, 19.4, 19.5, 19.6, 19.8, 21.7, 24.9, 25.0, 25.1, 28.3(0), 28.3(4), 28.4, 28.6, 28.6(5), 28.7 (8 carbons unresolved under here), 30.9, 40.9, 57.1, 60.5, 65.3, 66.8, 66.9, 71.4, 74.4, 79.0, 113.0, 126.0, 129.5, 157.3, 168.1, 168.6, 168.8, 168.9, 169.8, 171.3; *m*/*z* 819 (M + H^+). Found: C, 64.44, H, 8.60, N, 3.42%, $C_{44}H_{70}N_2O_{12}$ requires C, 64.52, H, 8.61, N, 3.42%.

N,N′-Dimethyl-2-[2,3,4,6-tetra-*O*-acetyl-β-D-galactopyranosyl-(1 → 4)-2,3,6-tri-*O*-acetyl-β-D-glucopyranosyl]-2-(4-octadecyloxybenzyl)malonamide (21)

Compound **21** (0.48 g, 71%); mp 137–138 °C (from acetonitrile); δ_H (400 MHz, $CDCl_3$) 0.81 (3H, t, *J* 6.7, $ArOCH_2CH_2$-$CH_2(CH_2)_{14}CH_3$), 1.19 (28H, br s, $ArOCH_2CH_2CH_2(CH_2)_{14}$-$CH_3$), 1.36 (2H, qnt, *J* 7.0, $ArOCH_2CH_2CH_2(CH_2)_{14}CH_3$), 1.67 (2H, qnt, *J* 7.0, $ArOCH_2CH_2CH_2(CH_2)_{14}CH_3$), 1.79 (3H, s, $OCOCH_3$), 1.91 (3H, s, $OCOCH_3$), 1.93 (3H, s, $OCOCH_3$), 2.00 (6H, s, 2 × $OCOCH_3$), 2.08 (3H, s, $OCOCH_3$), 2.09 (3H, s, $OCOCH_3$), 2.52 (3H, d, *J* 4.5, $NHCH_3$), 2.78 (3H, d, *J* 4.3, $NHCH_3$), 3.03 (1H, d, J_{AB} 13.3, CHH′Ar), 3.11 (1H, J_{AB} 13.3, CHH′Ar), 3.72 (2H, m, 4-H, 5-H), 3.82 (3H, m, $ArOCH_2CH_2$-$CH_2(CH_2)_{14}CH_3$, 5′-H), 4.01 (1H, dd, *J* 9.5, 11.1, 6′-H), 4.08 (1H, dd, *J* 5.0, 11.1, 6′-H′), 4.35 (1H, dd, *J* 2.6, 12.0, 6-H), 4.47 (3H, m, 1-H, 6-H′, 1′-H), 4.80 (1H, t, *J* 9.1, 2-H), 4.91 (1H, dd, *J* 3.0, 10.2, 3′-H), 5.06 (1H, dd, *J* 8.7, 10.2, 2′-H), 5.15 (1H, m, 3-H), 5.29 (1H, d, *J* 3.0, 4′-H), 6.65 (2H, d, J_{AB} 7.3, ArH), 6.82 (2H, d, J_{AB} 7.3, ArH), 6.87 (1H, q, *J* 4.5, $NHCH_3$), 9.14 (1H, q, *J* 4.3, $NHCH_3$); δ_C (100 MHz, $CDCl_3$) 14.5, 20.7, 20.9, 21.0(2 carbons unresolved under here), 21.0(5), 21.1, 21.4, 23.1, 26.3, 26.4, 26.7, 29.6, 29.7, 29.8, 29.9(5), 29.9(7), 30.0, 30.1 (7 carbons unresolved under here), 32.3, 42.2, 58.4, 61.1, 62.5, 66.9, 68.2, 69.5, 69.9, 71.1, 71.3, 74.5, 76.9, 78.2, 79.7, 101.1, 114.4, 127.2, 130.9, 158.7, 169.3, 169.7, 169.8, 170.1, 170.4, 170.5, 170.7, 171.4, 172.3; *m*/*z* 1107 (M + H^+). Found: C, 60.98, H, 7.90, N, 2.41%, $C_{56}H_{86}N_2O_{20}$ requires C, 60.74, H, 7.83, N, 2.53%.

BIAcore experiments

Preparing the sensor chip

An HPA sensor chip (from BIAcore, Sweden) was washed overnight at 25 °C with degassed, ultrafiltered 20 mM HEPES

buffer pH 7.0 (containing 90 mM NaCl) at a flow rate of 2 μl min^{-1}. The chip was then washed with 40 mM *n*-octyl β-D-glucopyranoside (Sigma, Dorset, UK) dissolved in buffer for 7 min at a flow rate of 5 μl min^{-1} immediately prior to deposition of the selected lipids. Dipalmitoyl phosphatidylcholine (Sigma, Dorset, UK) dissolved in chloroform–methanol (1 : 1 v/v) was mixed with varying amounts of the selected lactosyl thiooxaalkane or carboglycolipid in the same solvent to give solutions of 10, 15 and 25 mol% of glycolipid. A control of pure dipalmitoyl phosphatiylcholine was used. The solutions were evaporated under reduced pressure, dried for several hours over P_2O_5 in a vacuum dessicator, and then suspended in HEPES buffer by warming to 30 °C and vortexing to give a final concentration of phospholipid of 0.5 mM. Each of the four channels of the sensor chip was exposed for 3 h to a different concentration of glycolipid from 0 to 25 mol% at a flow rate of 2 μl min^{-1} and 35 °C, to allow the lipids to impregnate the existing thioalkyl layer attached to the gold surface by the manufacturers.

The chip surface was washed with a fast flow of buffer (100 μl min^{-1} for 5 min) to remove loosely adherent lipid, followed by two washes with 20 mM NaOH (5 μl min^{-1} for 5 min each) and then with buffer to stabilize the phospholipid monolayer.

Kinetic measurements (binding constants)

Low concentrations of RCA_{120} analyte (Sigma, Dorset,UK) 25, 50, 75, 100 and 150 nM were used to minimize bulk refractive index changes and possible mass transfer effects. Each solution was injected into all channels and channel 1 (the negative control of phospholipid) was subtracted from each channel (10 mol% glycolipid) to remove any bulk refractive index changes. Experiments were repeated at least five times. The results in Table 1 are the means of the k_a and k_d values derived from the sensorgram and the calculated values for K_A and K_D

The temperature was changed in random order to obtain the equilibrium constants for each compound at 5, 10, 15, 20, 25 and 30 °C

Acknowledgements

We thank Dr H. D. B. Jenkins, Department of Chemistry, University of Warwick for his helpful suggestions, particularly on the kinetic and thermodynamic work, during the preparation of this manuscript and Mr M. N. Willand who synthesised the thiolactosyl lipids.

References

1 A. Varki, *Glycobiology*, 1993, **3**, 97–130.
2 H.-C. Siebert, C.-W. von der Lieth, M. Gilleron, G. Reuter, J. Wittmann, J. F. G. Vleigenthart and H-J. Gabius, Carbohydrate–protein interaction, ch. 16 in *Glycosciences: Status and Perspectives*, ed. H-J Gabius and S. Gabius, Chapman and Hall, Weinheim, 1997, pp. 291–310.
3 S. Howard and S. G. Withers, *J. Am. Chem. Soc.*, 1998, **120**, 10326–10331.
4 Q. Wang, M. Wolff, T. Polat, Y. Du and R. J. Linhardt, *Bioorg. Med. Chem. Lett.*, 2000, **10**, 941–944.
5 C. Pasquarrello, S. Picasso, R. Demange, M. Malissard, E. G. Berger and P. Vogel, *J. Org. Chem.*, 2000, **65**, 4295–4260.
6 I. Riemann, M. A. Papadopoulos, M. Knorst and W-D. Fessner, *Aust. J. Chem.*, 2002, **55**, 147–154.
7 K-S. Ko, J. Kruse and N. L. Pohl, *Org. Lett.*, 2003, **5**, 1781–1783.
8 Y. Du, J. Linhardt and I. R. Vlahov, *Tetrahedron*, 1998, **54**, 9913–9959.
9 C. J. Li and T. H. Chan, *Tetrahedron*, 1998, **55**, 11149–11176.
10 F. Rodrigues, Y. Canac and A. Lubineau, *Chem. Commun.*, 2000, 2049–2050.
11 P. Critchley, M. N. Willand, A. K. Rullay and D. H. G. Crout, *Org. Biomol. Chem.*, 2003, **1**, 928–938.
12 W. J. Lees, A. Spaltenstein, J. E. Kingery-Wood and G. M. Whitesides, *J. Med. Chem.*, 1994, **37**, 3419–3433.
13 Y. C. Lee and R. T. Lee, *Acc. Chem. Res.*, 1995, **28**, 321–327.
14 N. Stahl, D. R. Borchelt and S. B. Prusiner, *Biochemistry*, 1990, **29**, 5405–5412.
15 L. V. Chernomordik, E. Leikina, M. M. Kozlov, V. A. Fralav and J. Zimmerberg, *Mol. Membrane Biol.*, 1999, **16**, 33–42.
16 C. W. M. Grant and M. W. Peters, *Biochim. Biophys. Acta*, 1984, **779**, 403–422.
17 N. Stromberg, P. G. Nyholm, I. Pascher and S. Normark, *Proc. Natl. Acad. Sci. USA*, 1991, **88**, 9340–9344.
18 A. Kiarash, B. Boyd and C. A. Lingwood, *J. Biol. Chem.*, 1994, **269**, 11138–11146.
19 R. J. Stewart and J. M. Boggs, *Biochemistry*, 1993, **32**, 5605–5614.
20 J. D. Andrade and V. Hlady, *Adv. Polym. Sci.*, 1986, **77**, 1–63.
21 N. Sanghera and T. J. T. Pinheiro, *J. Mol. Biol.*, 2002, **315**, 1241–1256.
22 E. Ostuni, L. Yan and G. M. Whitesides, *Colloids Surf. B*, 1999, **15**, 3–30.
23 M. Mammen, S-K. Choi and G. M. Whitesides, *Angew. Chem., Int. Ed.*, 1998, **37**, 2754–2794.
24 N. F. Burkhalter, S. M. Dimick and E. J. Toone, Protein–carbohydrate interaction: fundamental considerations, ch. 31 in *Carbohydrates in Chemistry and Biology*, ed. B. Ernst, G. W. Hart and P. Sinay, Wiley-VCH, Weinheim, 2000, Part 1, vol. 2, pp. 863–914.
25 M. C. Chervenak and E. J. Toone, *J. Am. Chem. Soc.*, 1994, **116**, 10533–10539.
26 C. R. MacKenzie and T. Hirama, *Methods Enzymol.*, 2000, **312**, 205–216.
27 R. U. Lemieux, *Acc. Chem. Res.*, 1996, **29**, 373–380.
28 H. Roos, R. Karlsson, H. Nilshans and A. Persson, *J. Mol. Recognit.*, 1998, **11**, 204–210.
29 J. W. Barton, M. Buhaenko, B. Moyle and N. M. Ratcliffe, *J. Chem. Soc., Chem. Commun.*, 1988, 488–489.
30 Y-F. Leu and C. K. Lai, *J. Chin. Chem. Soc. (Taipei)*, 1997, **44**, 89–91.
31 (*a*) V. Percec, C.-H. Ahn, W-D. Cho, A. M. Jamieson, J. Kim, T. Leman, M. Schmidt, M. Gerele, M. Möller, S. A. Prokhorova, S. S. Sheiko, S. Z. D. Cheng, A. Zhang, G. Ungar and D. J. P. Yeardley, *J. Am. Chem. Soc.*, 1998, **120**, 8619–8631; (*b*) V. Percec, W-D. Cho, P. E. Mosier, G. Ungar and D. J. P. Yeardley, *J. Am. Chem. Soc.*, 1998, **120**, 11061–11070.
32 M. A. Gonzalez, J. L. J. Requejo, A. Jimenez, J. C. P. Albarran and J. A. G. Perez, *Carbohydr. Res.*, 1986, **158**, 53–56.
33 (*a*) G. Clarkson and G. Wulff, *Carbohydr. Res.*, 1994, **257**, 81–95; (*b*) G. Clarkson and G. Wulff, *Makromol. Chem.*, 1994, **195**, 2603–2610.
34 B. S. Jursic, *Tetrahedron Lett.*, 2000, **41**, 5325–5328.
35 S. Shuto, Y. Yahiro, S. Ichikawa and A. Matsuda, *J. Org. Chem.*, 2000, **65**, 5547–5557.
36 P. G. Goekjian, T-C. Wu and Y. Kishi, *J. Org. Chem.*, 1991, **56**, 6412–6422.
37 N. Boden, R. J. Bushby, S. Clarkson, S. D. Evans, P. F. Knowles and A. Marsh, *Tetrahedron*, 1997, **53**, 10939–10952.
38 R. A. Bartsch, C. V. Cason and B. P. Czech, *J. Org. Chem.*, 1989, **54**, 857–860.
39 T. W. Greene and P. G. M. Wuts, in *Protective Groups in Organic Synthesis*, Wiley, New York. 2nd edn., 1991.
40 M. Elofsson, S. Roy, B. Walse and J. Kihlberg, *Terahedron Lett.*, 1991, **32**, 7613–7616.
41 F. Wilhelm, S. K. Chatterjee, B. Rattay, P. Nuhn, R. Benecke and J. Ortwein, *Leibigs Ann. Chem.*, 1995, **9**, 1673–1679.
42 R. Karlsson, A. Michaelsson and L. Mattsson, *J. Immunol. Methods*, 1991, **145**, 229–249.
43 P. Harder, M. Grunze, R. Dahint, G. M. Whitesides and P. E. Laibinis, *J. Phys. Chem. B*, 1998, **102**, 426–436.
44 F. P. Schwarz, K. D. Puri, R. G. Bhat and A. Surolia, *J. Biol. Chem.*, 1993, **268**, 7668–7677.
45 A. Surolia, N. Sharon and F. P. Schwarz, *J. Biol. Chem.*, 1996, **271**, 17697–17703.
46 G. Zeder-Lutz, E. Zuber, J. Witz and M. H. V. van Regenmortel, *Anal. Biochem.*, 1997, **246**, 123–132.
47 J. Deinum, L. Gustavsson, E. Gyzander, M. Kullman-Magnusson, A. Edstrom and R. Karlsson, *Anal. Biochem.*, 2002, **300**, 152–162.
48 M. Mammen, E. J. Shakhnovich, J. M. Deutch and G. M. Whitesides, *J. Org. Chem.*, 1998, **63**, 3821–3830.
49 M. Mammen, E. J. Shakhnovich and G. M. Whitesides, *J. Org. Chem.*, 1998, **63**, 3168–3175.
50 J. Lahiri, L. Isaacs, B. Grzybowski, J. D. Carbeck and G. M. Whitesides, *Langmuir*, 1999, **15**, 7186–7198.
51 L. Chen, M. L. Johnson and R. L. Biltonen, *Biophys. J.*, 2001, **80**, 254–270.
52 S. Sharma, S. Bharadwaj, A. Surolia and S. K. Podder, *Biochem. J.*, 1998, **333**, 539–542.